

See discussions, stats, and author profiles for this publication at: <https://www.researchgate.net/publication/231274514>

The Modified Yen Model†

ARTICLE *in* ENERGY & FUELS · JANUARY 2010

Impact Factor: 2.79 · DOI: 10.1021/ef900975e

CITATIONS

230

READS

222

1 AUTHOR:



[Oliver C Mullins](#)

Schlumberger Limited

244 PUBLICATIONS 5,953 CITATIONS

[SEE PROFILE](#)

The Modified Yen Model[†]

Oliver C. Mullins*

Schlumberger-Doll Research, Cambridge, Massachusetts 02139

Received September 2, 2009. Revised Manuscript Received November 24, 2009

Asphaltenes, the most aromatic of the heaviest components of crude oil, are critical to all aspects of petroleum use, including production, transportation, refining, upgrading, and heavy-end use in paving and coating materials. As such, efficiency in these diverse disciplines mandates proper chemical accounting of structure–function relations of crude oils and asphaltenes, the vision of petroleomics (*Asphaltenes, Heavy Oils and Petroleomics*; Mullins, O. C., Sheu, E. Y., Hammami, A., Marshall, A. G., Eds.; Springer: New York, 2007). Indeed, the molecular characterization of asphaltenes is required as well as the detailed understanding of the hierarchical colloidal structures of asphaltenes and petroleum. With great prescience, Professor Teh Fu Yen and co-workers proposed a hierarchical model of asphaltenes to account for many of their characteristics known at that time (Dickie, J. P.; Yen, T. F. Macrostrucutres of asphaltic fractions by various instrumental methods. *Anal. Chem.* 1967, 39, 1847–1852). This model is rightfully known as the Yen model. Nevertheless, at the time the Yen model was formulated, there were many order-of-magnitude uncertainties in asphaltene science that precluded establishing structure–function relations and causality, thereby rendering the Yen model somewhat phenomenological. Petroleum science has advanced greatly in recent years enabling development of a much more specific model yet still based on precepts of the Yen model; we call this the “modified Yen model”. The modified Yen model is shown to account for wide ranging, myriad properties of asphaltenes, including their dynamics. In addition, the modified Yen model has even proven successful for understanding interfacial phenomena involving asphaltenes. Moreover, the modified Yen model accounts for fundamental observations in oil reservoirs and is now propelling significantly improved efficiency in oil production. The modified Yen model is a simple, yet powerful construct that provides the foundation to test future developments in asphaltene and petroleum science; refinement of the modified Yen model is an expected outcome of this process.

1. Introduction

Asphaltenes play a central role in the use of petroleum resources. Asphaltenes strongly affect viscosity, which impacts all areas of resource exploitation. In the production of oil, asphaltene distributions have proven to be useful for reservoir characterization and risk management. Asphaltenes can alter wettability of rock, such as in mixed wettability carbonate reservoirs in the Middle East, thereby strongly impacting recovery. Likewise, asphaltenes, especially within a surface science context, must be considered in enhanced oil recovery. Reservoir tar mats are largely asphaltenes and have a huge impact on field development plans. Asphaltene phase transitions are a well-known flow assurance problem, and common emulsion stability problems are caused in large part by asphaltenes. Asphaltenes are hydrogen-deficient compared to liquid hydrocarbons; therefore, upgrading the massive heavy oil and bitumen deposits around the world requires either removing the asphaltene fraction or hydrogenating it. In addition, of course, the strongly temperature-dependent rheological properties of asphaltenes make them particularly useful as paving and coating materials. Asphaltenes are also important regarding environmental concerns; indeed, asphaltenes are the most refractory component of crude oil and thus very important in ecological settings. Man-made oil spills can be

environmentally pernicious because of the sudden increase of large volumes of crude oil. In volumetric terms, natural oil seeps dwarf the man-made release of crude oil into the environment. As a result, asphaltene derivatives are present in the world's oceans in significant quantity and must be understood within the context of the global carbon cycle.

The importance of asphaltenes is unquestioned. Nevertheless, there is a complexity when addressing asphaltenes. Their chemical identity has been obscured; consequently, asphaltenes are defined as a solubility class. For example, a common asphaltene definition is the *n*-heptane-insoluble, toluene-soluble component of a crude oil or carbonaceous material. There has been tremendous scientific focus on these materials as gleaned from an incomplete listing of books featuring asphaltenes, treating all manners of asphaltene properties, including molecular structure, colloidal properties, interfacial properties, and chemical reactivity.^{1–8} At a fairly early stage,

(1) *Asphaltenes, Heavy Oils and Petroleomics*; Mullins, O. C., Sheu, E. Y., Hammami, A., Marshall, A. G., Eds.; Springer: New York, 2007.

(2) Dickie, J. P.; Yen, T. F. Macrostrucutres of asphaltic fractions by various instrumental methods. *Anal. Chem.* 1967, 39, 1847–1852.

(3) Yen, T. F. Asphaltic materials. In *Encyclopedia of Polymer Science and Engineering*, 2nd ed.; Mark, H. S., Bikales, N. M., Overberger, C. G., Menges, G., Eds.; John Wiley and Sons: New York, 1989; Supplementary Volume, pp 1–10.

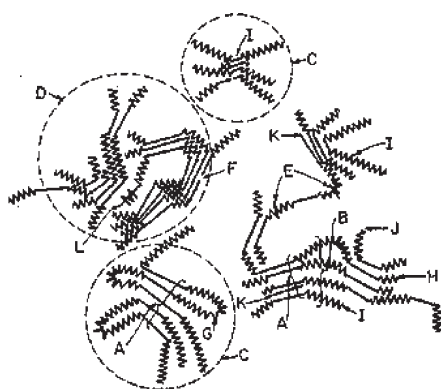
(4) *Structures and Dynamics of Asphaltenes*; Mullins, O. C., Sheu, E. Y., Eds.; Plenum Press: New York, 1998.

(5) *Asphaltenes, Fundamentals and Applications*; Sheu, E. Y., Mullins, O. C., Eds.; Plenum Press: New York, 1995.

(6) Sharma, M. K.; Yen, T. F. *Asphaltene Particles in Fossil Fuel Exploration, Recovery, Refining, and Processing Processes*; Springer: New York, 1994.

* Presented at the 10th International Conference on Petroleum Phase Behavior and Fouling.

† To whom correspondence should be addressed. E-mail: mullins1@slb.com.

**Figure 1.** Macrostructure of asphaltenes

- A. Crystallite B. Chain bundle
 C. Particle D. Micelle
 E. Weak link F. Gap and hole
 G. Intrachuster H. Intercluster
 I. Resin J. Single layer
 K. Petroporphyrin L. Metal

Figure 1. Yen model from Professor Teh Fu Yen, as proposed in 1967.²

Professor Teh Fu Yen codified the field of asphaltene science by providing a hierarchical picture of asphaltenes (cf. Figure 1).² In addition to providing a framework for comparison of new results, the “Yen model” related structures of different length scales, allowing a broader comprehension of the utility of results within a given length scale. Refinements of the Yen model have continued to be made.³ The Yen model has been very useful for most contributors in the field and has become an intrinsic component of much analysis.

Nevertheless, at the time of the original proposition of the Yen model² and indeed at the time of more recent expositions,³ there were many large and fundamental debates in asphaltene and petroleum science that precluded a first principles approach to the Yen model. These numerous debates were often at least an order of magnitude in scale and proved a lack of any consensus in the field. We list the subjects and scale of these debates in Table 1, comparing the perspective only a decade ago versus today. Indeed, the uncertainty in the most basic issue, asphaltene molecular weight, was enormous. Ten years ago, there was not only huge disagreement, but in addition, there were very few who supported the currently accepted value for asphaltene molecular weight. Without resolution of this key molecular attribute, structure–function relationships are precluded, petroleomics becomes only wishful thinking, and phenomenology prevails.

Asphaltene science has progressed dramatically in the last 10 years, as depicted in Table 1, and indeed, this is the primary reason that motivated writing a recent book on asphaltenes¹ with 46 contributing scientists. Table 1 is very extensive; for some topics, there is more certainty, while others, less so. Each topic will be treated below to provide a general understanding of the corresponding current status. First, a brief description of the modified Yen model is given: extensive referencing is provided in subsequent sections.

2. Modified Yen Model

As a consequence of this tremendous improvement in the understanding of asphaltenes, we propose a much more

refined description of asphaltenes, “the modified Yen model”. The modified Yen model consists of a first-principles approach in treating the hierarchical structures of and properties manifested by asphaltenes. As such, the asphaltene molecular structures are absolutely key. The modified Yen model is shown in Figure 2; we emphasize the different asphaltene hierarchical structures and will show how the hierarchical structures are related in terms of structure and energies. The predominant asphaltene molecular architecture is shown in Figure 2, with its single, moderate-sized polycyclic aromatic hydrocarbon (PAH) ring system with peripheral alkane substituents. These molecules can form asphaltene nanoaggregates with a single, disordered stack of PAHs and with aggregation numbers ~6. The exterior of the nanoaggregate is dominated by the alkane substituents. These nanoaggregates can form *clusters* of nanoaggregates. These asphaltene nanoaggregate clusters are not much bigger than the nanoaggregates, and aggregation numbers are estimated to be eight nanoaggregates. We now explore each component of the modified Yen model in greater detail.

The predominant but not only asphaltene molecular architecture, as shown in Figure 3, consists of a single, somewhat large PAH with cycloalkane, branched- and straight-chain substituents. There is often heteroatom content; asphaltene nitrogen is entirely contained within the PAH in pyrrolic structures and to a lesser extent pyridinic structures. Some sulfur is thiophenic, thus contained in the PAH, and the rather small oxygen content appears in various groups, with some likely phenolic. There are very few charged species in asphaltenes; there are simply very few sites that can support charge. Even the asphaltene metalloporphyrins, which are present in low concentration, are charge-neutral (but they do possess some charge separation). Consequently, charged groups contribute very little to the energetics of asphaltenes.

The PAH is the primary site of intermolecular attraction. It is polarizable; thus, the PAH is the site of induced dipole–induced dipole interactions. In large measure, this interaction increases monotonically with the number of fused rings and thus is significant for the somewhat large PAHs of asphaltenes. In addition, the PAH possesses a degree of charge separation primarily associated with the heteroatoms, for example, giving rise to dipole–dipole interactions. Consequently, the well-known aggregation tendencies of asphaltenes are driven by the PAH. Nevertheless, the energy of the dipole–dipole interaction and induced dipole–induced dipole interaction decreases with the separation distance r as r^6 ; asphaltene attractive interactions are very short-range. In contrast, the peripheral substituents are predominantly alkane (including cycloalkane). These groups create steric hindrance, preventing close approach of the attractive PAHs embedded in the molecular interior.

Asphaltenes are a solubility class; there is a balance of attractive and repulsive forces between and among asphaltene molecules. If the intermolecular attraction was too great, the molecules would not dissolve in toluene and thus not be asphaltene; coronene with its seven-fused rings has sparing solubility in toluene. If the attraction were too little (or steric repulsion too great), then the molecules would dissolve in *n*-heptane and thus not be asphaltene. There are several implications of this freshman chemistry model for asphaltenes (PAH attraction in the molecular interior and steric repulsion on the periphery). If the alkanes are cracked off the PAHs, then the attractive forces are no longer balanced by repulsion and an insoluble solid, coke, forms. If the source material does

(7) *Chemistry of Asphaltenes*; Bunger, J. W., Li, N. C., Eds.; American Chemical Society: Washington, D.C., 1981.

(8) *Bitumens, Asphalts and Tar Sands*; Chillingarian, G. V., Yen, T. F., Eds.; Elsevier Scientific Publishing Co.: New York, 1978.

Table 1. Resolution of Numerous Issues in Asphaltene Science during the Last 10 Years

scientific issue	range of reported values in ~1998	values in 2009	width of distribution in 2009
asphaltene molecular weight	less than 1000 to 1000000000 Da	750 Da	400–1000 full width at half-maximum (fwhm)
number of polycyclic aromatic hydrocarbons (PAHs) in an asphaltene molecule	1–20	1 dominates	small mass fraction with 0, 2, 3, etc.
number of fused rings per asphaltene PAH	2–20	7	ring systems
number of PAH stacks in asphaltene nanoaggregate	unknown	1	4–10
aggregation number of nanoaggregates	10–100	< 10	4–10
critical nanoaggregate concentration of asphaltenes	50 mg/L to 5 g/L	100 mg/L	50–150 mg/L
concentration of cluster formation size of cluster	unknown	~3 g/L	2–5 g/L
role of resins in asphaltene nanoaggregate	none to necessary	6 nm for small clusters	likely also larger clusters dependent upon the temperature and concentration
relation of nanoaggregate to cluster	unknown	~15% of crude oil nanoaggregates are resins; resins not surfactant	depends upon definitions
relation of nanoaggregates in toluene to those in crude oil	unknown	clusters consist of nanoaggregates very similar in size and composition	

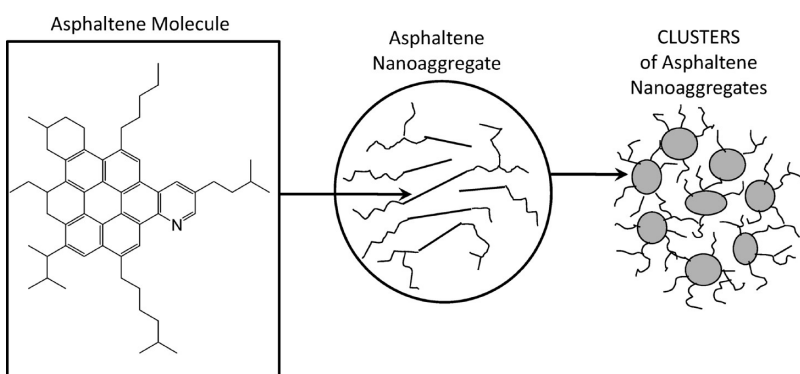


Figure 2. Modified Yen model. (Left) The predominant asphaltene molecular architecture has a single, moderately large PAH with peripheral alkanes. (Center) Asphaltene molecules form asphaltene nanoaggregates with aggregation numbers of ~6 and with a single disordered stack in the interior with peripheral alkane. (Right) Asphaltene nanoaggregates can form clusters with aggregation numbers estimated to be ~8. The modified Yen model provides a framework to treat large numbers of diverse asphaltene studies.

not have much alkane carbon, such as coal-derived asphaltenes, then the corresponding PAHs must be smaller. The smaller ring systems and less alkane carbon cause the coal-derived asphaltenes to have a much smaller molecular weight than their petroleum asphaltene cousins (the coal-derived asphaltenes of interest here are from coal liquefaction, with subsequent refining with resid formation. The coal-derived asphaltenes from this process do not have much heteroatom content and are similar in this context to virgin petroleum asphaltenes).

An important implication of asphaltene molecular structure is that aggregation numbers of colloidal asphaltenes are predicted to be very small. After several molecules (nano)-aggregate, their alkanes distort to occupy reduced available volume. Thus, after several asphaltene molecules aggregate, the nanoaggregate projects primarily the steric-repelling alkanes to the outside world (a hairy tennis ball) and additional asphaltene molecules are not able to achieve close approach to the interior PAHs. Thus, additional asphaltene molecules form new nanoaggregates of small aggregation numbers and not large nanoaggregates. The asphaltene “critical nanoaggregate concentration” (CNAC) is the concentration at which further nanoaggregate growth shuts off. At concentrations lower than the CNAC, asphaltenes form dimers and other small multimers as a buildup to the nanoaggregate. Figure 4 provides a cross-sectional view of the asphaltene nanoaggregates. The dimensions are ~2 nm; subtleties about what this

and other lengths really mean will be discussed below. The straight thick line segments represent the (single) PAH in each of the molecules, while the thinner crooked segments represent the alkane (including cycloalkane) substituents. The individual PAHs are *not* covalently cross-linked to each other.

These nanoaggregates are fairly tightly bound, with a binding energy estimated to be a few kilojoules per mole. They are formed when asphaltenes are placed in toluene in sufficient concentration. They do not need resins to form or to be stably suspended. Crude oils possess nanoaggregates very similar in nature to the nanoaggregates formed when asphaltenes are added to toluene. These crude oil nanoaggregates are stable at reservoir temperatures (~100 °C). Nevertheless, in crude oils, resins are present; the heaviest and only the heaviest resins participate in the aggregation at a level of ~15% mass fraction (which naturally depends upon the exact separation method used to define asphaltenes and resins). With such small nanoaggregates and relatively small resin fraction, resins do not act as classic surfactants for these asphaltene nanoaggregates.

The asphaltene solubility classification of toluene soluble captures the most aromatic of the heaviest components in crude oils. The *n*-heptane insolubility captures most but not all of that fraction that self-assembles in crude oil into nanoaggregates. If *n*-pentane is used to define asphaltenes, a greater fraction is captured of the crude oil components that self-assemble into nanoaggregates; however, there is also an increase in capturing components that do not self-assemble in

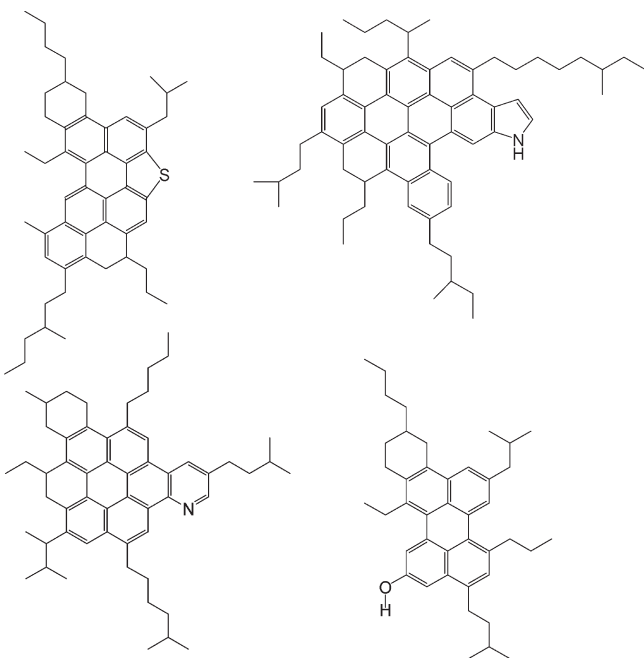


Figure 3. Proposed asphaltene molecular structures. These structures are consistent with the many molecular constraints that are now known to apply to the asphaltenes. These are the types of molecular structures that dominate asphaltenes.

crude oil. If other carbonaceous materials, such as coal-derived materials, are used to obtain asphaltenes, then the chemical identity of the asphaltenes is somewhat different from that of petroleum asphaltenes; however, the hierarchical aggregation properties of these different asphaltenes are similar to those of the petroleum asphaltenes. Not surprisingly, the solubility classification of asphaltenes captures materials of similar aggregation characteristics but not necessarily identical chemistries for different source materials.

The asphaltene nanoaggregates can cluster in crude oils and toluene. There is some uncertainty about the full range of size of the clusters; nevertheless, the clusters are bounded by the nanoaggregates ~ 3 nm and the smallest flocs (~ 300 nm) (asphaltene flocs are formed and phase separate when asphaltenes are sufficiently destabilized in solution). The clusters are most likely fractal, and the smallest type of clusters is ~ 6 nm. Figure 5 provides a conceptual view of the clusters. The gray circles represent the aromatic core of the asphaltene nanoaggregates, while the crooked lines represent the nanoaggregate alkane substituents. The different aromatic cores are not covalently cross-linked. The binding energy is rather small, and the clustering can be strongly impacted by changing temperature, concentration, and liquid-phase properties. Indeed, the enormous rheological dependence of asphaltenes on temperature and concentration is in part due to variable clustering.

The length scale of the smallest type of clusters is ~ 6 nm, and these can remain stably (but delicately) suspended in crude oil for geologic time. It is plausible that larger clusters can form with a length scale of tens of nanometers and larger. If asphaltene instability continues to increase, flocs form and phase separate. Smaller flocs are on order $1\ \mu\text{m}$ and can grow to macroscopic size.

The hierarchical structure of asphaltenes and thus the modified Yen model is relevant for all aspects of crude oil and asphaltene properties, including bulk rheology, oil field distributions of asphaltenes, phase stability of asphaltenes and crude oils, and interfacial properties. The modified Yen model

provides a framework to analyze a tremendous volume of data at multiple length scales for these materials. Below, the foundations of the modified Yen model are justified.

3. Asphaltene Molecular Architecture

3.1. Asphaltene Molecular Weight. The molecular weight of asphaltenes had been a huge controversy for decades. At this juncture, the main features of the debate are essentially resolved; nevertheless, details of the distribution are still being sorted out, and as always, new techniques are informative. This topic remained a substantial debate for a long time for several reasons. Asphaltenes are polydisperse at the molecular level, causing application of any technique to be somewhat uncertain; any technique used to measure asphaltene molecular weight has shortcomings, known and sometimes unknown and often debilitating. Consequently, the same methods applied to the same samples can give different results by one or more orders of magnitude. In addition, asphaltenes associate at different concentrations with different binding energies (cf. section 2). The previously unknown extent and nature of asphaltene aggregation caused limitations in some methods to go unrecognized. Other sources of confusion also had contributed to keep this controversy alive. Indeed, the central role of asphaltene molecular weight in the field motivated its measurement in almost all laboratories; unfortunately, the measurement is difficult, and some laboratories were correspondingly ill-equipped. Fortunately, the issue is now largely resolved; without resolution of asphaltene molecular weight, determination of structure–function relations is greatly retarded, the modified Yen model would be precluded, and the field of asphaltene science would be reduced in great measure to phenomenology.

Molecular Diffusion. Diffusion measurements of asphaltene molecules played a decisive role in resolving the molecular-weight controversy. There are two primary methods used to measure asphaltene molecular weight, mass spectrometry and molecular diffusion. Other techniques have been employed but suffer debilitating effects from asphaltene aggregation, as will be discussed. Unlike the mass spectrometry measurements, the molecular diffusion measurements on asphaltenes always give a consistent picture. The first molecular diffusion measurements performed on asphaltenes employed time-resolved fluorescence depolarization (TRFD).^{9–15} TRFD employs a polarized excitation laser to excite the molecular ensemble thus becoming polarized in the lab frame. Absorption of polarized photons from the laser beam yields correspondingly polarized excited electronic states of the absorber molecules. For any molecule, the

(9) Groenin, H.; Mullins, O. C. Asphaltene molecular size and structure. *J. Phys. Chem. A* **1999**, *103*, 11237–11245.

(10) Groenin, H.; Mullins, O. C. Molecular sizes of asphaltenes from different origin. *Energy Fuels* **2000**, *14*, 677.

(11) Buenrostro-Gonzalez, E.; Groenin, H.; Lira-Galeana, C.; Mullins, O. C. The overriding chemical principles that define asphaltenes. *Energy Fuels* **2001**, *15*, 972.

(12) Groenin, H.; Mullins, O. C.; Eser, S.; Mathews, J.; Yang, M.-G.; Jones, D. Asphaltene molecular size for solubility subfractions obtained by fluorescence depolarization. *Energy Fuels* **2003**, *17*, 498.

(13) Badre, S.; Goncalves, C. C.; Norinaga, K.; Gustavson, G.; Mullins, O. C. Molecular size and weight of asphaltene and asphaltene solubility fractions from coals, crude oils and bitumen. *Fuel* **2006**, *85*, 1.

(14) Buch, L.; Groenin, H.; Buenrostro-Gonzalez, E.; Andersen, S. I.; Lira-Galeana, C.; Mullins, O. C. Effect of hydrotreatment on asphaltene fractions. *Fuel* **2003**, *82*, 1075.

(15) Groenin, H.; Mullins, O. C. Asphaltene molecular size and weight by time-resolved fluorescence depolarization. In *Asphaltenes, Heavy Oils and Petroleomics*; Mullins, O. C., Sheu, E. Y., Hammami, A., Marshall, A. G., Eds.; Springer: New York, 2007; Chapter 2.

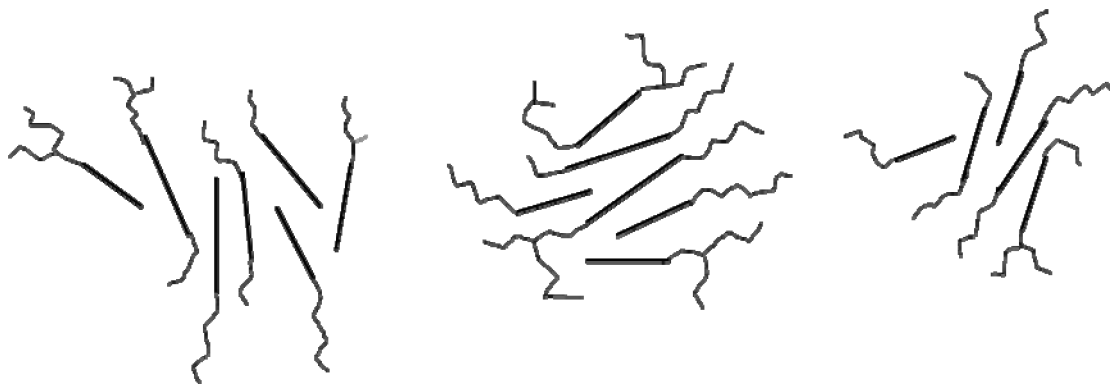


Figure 4. Asphaltene nanoaggregates. The aggregation number is ~6; each molecule has a PAH (depicted as a thick straight line) and alkane (and cycloalkane) peripheral substituents (depicted as lighter crooked lines). The individual PAHs are not covalently cross-linked in the nanoaggregates. One disordered PAH stack resides in the interior, and alkane is dominant in the nanoaggregate exterior.

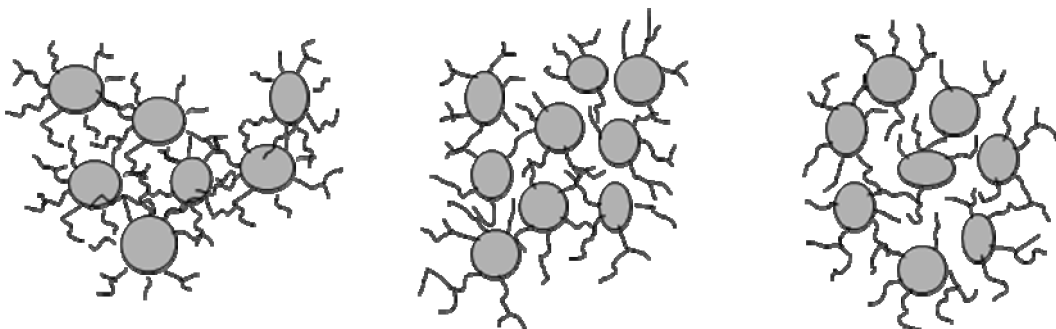


Figure 5. Clusters of nanoaggregates. Each gray circle represents the single PAH disordered “stack” in a nanoaggregate. The crooked lines represent the peripheral alkane substituents of the nanoaggregate.

(electric vector) polarization of the excited electronic state is tightly coupled to the molecular framework. As the molecule undergoes rotational random walk (rotational diffusion), the polarization direction continuously reorients. For an ensemble, the polarization decays. The rotational correlation time is the time that it takes for the molecule to reorient on the order of 1 rad. The measured rotational correlation time depends upon the shape of the molecule as well as its size, and particularly, for large molecules, internal rotation can yield somewhat shorter correlation times than expected for the molecule as a whole.

Figure 6 shows typical TRFD data for petroleum asphaltenes. The rotational correlation times are short and consistent with a most probable molecular weight of 750 Da. When the fluorescence and optical absorption spectra were analyzed, an estimate of the width of the distribution is given as 500–1000 Da.^{9–15} The long axis (diameter) of the asphaltene molecules ranges from 1.2 to 2.4 nm, with a presumed aspect ratio of 2. TRFD is necessarily limited to the fraction of asphaltenes that undergoes fluorescence. It is known that the fluorescence quantum yields of asphaltenes and crude oil fluorophores obey the well-known energy gap law;¹⁶ thus, the red-emitting fluorophores have small quantum yield.¹⁷ The TRFD experiments select specific excitation and emission wavelengths, enabling sensitive optics to measure very small quantum yield components. For reasons to be discussed below, coal-derived asphaltenes are found to be much smaller by TRFD (< 500 Da).

Results in close agreement with the TRFD measurements on coal-derived asphaltenes were reported using Taylor dispersion (TD).¹⁸ A small quantity of asphaltene is charged into a capillary followed by initiation of laminar flow. The initial asphaltene charge is distorted into a parabola. Larger diffusion constants remove asphaltene from both extreme ends of the parabolic flow, thereby reducing the spread, while smaller diffusion constants preclude asphaltene departure from the parabola, thereby maintaining the growing parabolic spread in laminar flow. TD relies on performing optical *absorption* measurements to monitor asphaltene spreading and, thus, is sensitive to the molecular fraction of asphaltenes with a PAH. In addition, TD is sensitive to translational diffusion and not rotational diffusion; the excellent agreement between TRFD and TD indicates that (1) the fluorescent asphaltenes are similar to the nonfluorescent asphaltenes and (2) the TRFD results are not distorted from possible internal rotational effects of molecules. Nuclear magnetic resonance (NMR) diffusion measurements confirm the very short translational diffusion times of asphaltene molecules and, of course, are sensitive to the asphaltene fraction with hydrogen.^{19,20} The TRFD and

(18) Wargadalam, V. J.; Norinaga, K.; Iino, M. Size and shape of a coal asphaltene studied by viscosity and diffusion coefficient measurements. *Fuel* 2002, 81, 1403–1407.

(19) Freed, D. E.; Lisitza, N. V.; Sen, P. N.; Song, Y. Q. Asphaltene molecular composition and dynamics from NMR diffusion measurements. In *Asphaltenes, Heavy Oils and Petroleomics*; Mullins, O. C., Sheu, E. Y., Hammami, A., Marshall, A. G., Eds.; Springer: New York, 2007; Chapter 11.

(20) Freed, D. E.; Lisitza, N. V.; Sen, P. N.; Song, Y. Q. A study of asphaltene nanoaggregation by NMR. *Energy Fuels* 2009, 23, 1189–1193.

(16) Turro, N. J. *Modern Molecular Photochemistry*; Benjamin/Cummings: Menlo Park, CA, 1978.

(17) Ralston, C. Y.; Wu, X.; Mullins, O. C. Quantum yields of crude oils. *Appl. Spectrosc.* 1996, 50, 1563.

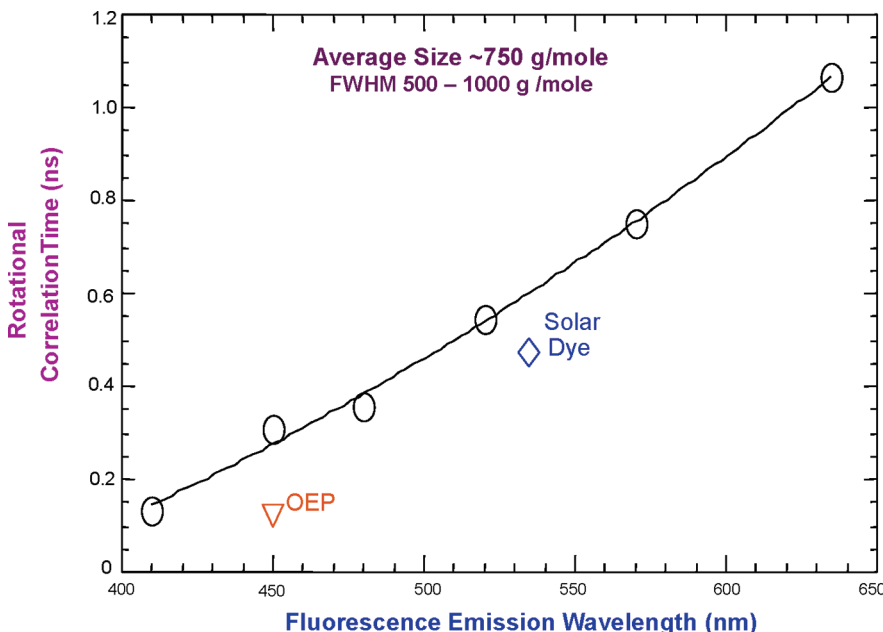


Figure 6. Rotational correlation times of asphaltene molecules as a function of their PAH fluorescence emission wavelength.^{9,10} Also shown are two model compounds: solar dye has a molecular weight of 755 Da, and octaethylporphine (OEP) has a molecular weight of 535 Da. All correlation times are small, indicating that asphaltene molecules are not large and are comparable to the model compounds. As will be discussed below, the large wavelength dependence of the correlation times indicates that the fluorophore is a major portion of the asphaltene molecule; thus, there is one PAH per asphaltene molecule.^{9,10}

NMR measurements obtained similar results on the same asphaltene samples, although the NMR diameters are slightly higher than those from TRFD; the NMR measurements give an average size (diameter) of 2.4 nm, presuming a sphere. As stated by the authors, the NMR measurements cannot go to very low concentrations (≥ 50 mg/L) and may have been perturbed by some di- and trimer concentrations.^{19,20}

Fluorescence correlation spectroscopy (FCS) was performed on ultra-dilute solutions of asphaltenes.^{21–23} In FCS, confocal optics focuses a laser into a cubic micrometer of solution. As (asphaltene) fluorophores diffuse into and out of the interrogated cubic micrometer, the fluorescence signal increases and decreases. When the decay time of the autocorrelation function of the fluorescence intensity is measured, the translational diffusion constant is obtained. Again, results in close agreement with other diffusion measurements were obtained by FCS. In particular, the much smaller size of coal-derived asphaltenes versus petroleum asphaltenes was found by FCS similar to TRFD. All four molecular diffusion measurements are in good agreement; asphaltenes are comprised of small molecules.

Mass Spectrometry (MS). MS naturally provides essential measurements in any study of molecular weight. After some difficulties, all methods of MS of asphaltenes are now providing consistent and vital results in asphaltene science. At an early stage, field ionization MS was applied to asphal-

tenes, giving the most probable molecules weight ≤ 1000 Da.²⁴ At the time, this result was not generally accepted; there were concerns about fragmentation and about not volatilizing the heaviest molecules. After some time, laser desorption ionization (LDI) MS and the closely related matrix-assisted laser desorption ionization MALDI MS were applied to asphaltenes. A huge problem emerged, in that different workers obtained very divergent results. LDI on vacuum resid asphaltenes (which we now know to be smaller than virgin crude oil asphaltenes¹⁴) gave a most probable molecular weight of ~ 450 Da.²⁵ LDI on virgin crude oil asphaltenes gave ~ 1000 Da²⁶ (although others in the same group obtained much higher numbers for the same samples!¹²). Other groups employing LDI on asphaltenes reported much higher molecular weights, such as $\sim 10\,000$ for a significant fraction of the asphaltenes.²⁷

Fortunately, the divergence of LDI results on asphaltenes has been resolved with new experiments and new experimental techniques.²⁸ Careful examination of the dependence of measured “molecular weights” on laser power, sample surface concentration, and even timing of ion collection

(21) Andrews, A. B.; Guerra, R.; Mullins, O. C.; Sen, P. N. Diffusivity of asphaltene molecules by fluorescence correlation spectroscopy. *J. Phys. Chem. A* **2006**, *110*, 8095.

(22) Guerra, R.; Andrews, A. B.; Mullins, O. C.; Sen, P. N. Diffusivity of coal and petroleum asphaltene monomers by fluorescence correlation spectroscopy. *Fuel* **2007**, *86*, 2016–2020.

(23) Schneider, M.; Andrews, A. B.; Mitra-Kirtley, S.; Mullins, O. C. Asphaltene molecular size from translational diffusion constant by fluorescence correlation spectroscopy. *Energy Fuels* **2007**, *21*, 2875–2882.

(24) Boduszynski, M. M. In *Chemistry of Asphaltenes*; Bunger, J. W., Li, N. C., Eds.; American Chemical Society: Washington, D.C., 1981; Chapter 7.

(25) Miller, J. T.; Fisher, R. B.; Thiagarajan, P.; Winans, R. E.; Hunt, J. E. Subfractionation and characterization of Mayan asphaltene. *Energy Fuels* **1998**, *12*, 1290.

(26) Yang, M.-G.; Eser, S. *Prepr. Symp.—Am. Chem. Soc., Div. Fuel Chem.* **1999**, *44*, 768.

(27) Herod, A. A.; Bartle, K. D.; Kandiyoti, R. Comment on a paper by Mullins, Martinez-Haya, and Marshall “Contrasting perspective on asphaltene molecular weight. This Comment vs the overview of A. A. Herod, K. D. Bartle, and R. Kandiyoti”. *Energy Fuels* **2008**, *22*, 4312–4317.

(28) Mullins, O. C.; Martinez-Haya, B.; Marshall, A. G. Contrasting perspective on asphaltene molecular weight. This Comment vs the overview of A. A. Herod, K. D. Bartle, R. Kandiyoti. *Energy Fuels* **2008**, *22*, 1765–1773.

showed conclusively that large asphaltene plasma densities result in gas-phase aggregation.^{29–32} Thus, low plasma densities especially at the ion collection times are required to obtain accurate asphaltene molecular weights.^{29–32} This important work obtained most probable asphaltene molecular weights of ~500 Da and was confirmed by novel LDI experiments. Instead of using a single laser to desorb and ionize the asphaltenes, two separate lasers are employed; an infrared (IR) laser desorbs the asphaltene, and a second ultraviolet (UV) laser performs the ionization step. The neutral plume of asphaltenes following the IR pulse desorption has a much smaller tendency to aggregate than the ionized asphaltenes in the plasma of standard LDI measurements. As such, much higher laser peak powers can be used to make sure all mass fractions of asphaltenes are being desorbed.^{33,34} Figure 7 shows that the molecular-weight distribution of asphaltenes is independent of the IR laser power, UV laser power, surface concentration of asphaltenes, or timing of ion collection.^{33,34} Most probable asphaltene molecular weights obtained by this method are ~600 Da. Atmospheric pressure photoionization (APPI) and atmospheric pressure chemical ionization (APCI) measurements have obtained average asphaltene molecular weights between 500 and 800 Da.³⁵ APPI ionizes both polar and nonpolar aromatics.³⁵ These results are in close agreement with other APCI measurements.³⁶ Field desorption MS has given somewhat higher values of ~1000 Da as the most probable molecular weight.³⁷ Very recently, a new method of MS has weighed in the debate, laser-induced acoustic desorption electron impact (LIAD-EI) MS.³⁸ In this method of desorption, asphaltenes are placed on a thin metal target. A laser is fired on the back side of the target, and an acoustic wave in the target causes the asphaltenes to go into the gas phase.³⁸ Much larger organics than the asphaltenes are shown to be detectable by

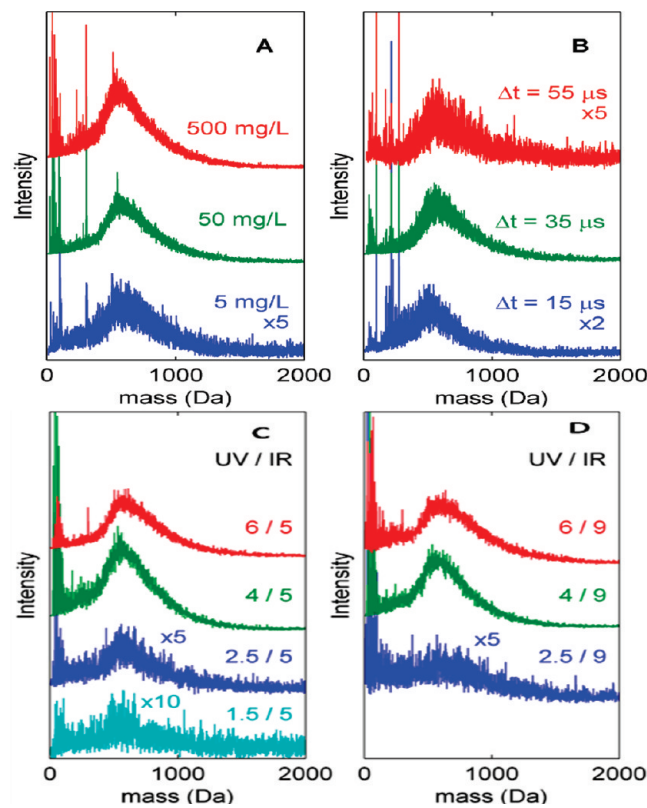


Figure 7. Two-step laser MS of asphaltenes.^{33,34} An IR laser is used to desorb the asphaltenes, and a UV laser is used to ionize the asphaltenes, thereby decoupling these two steps in LDI MS of asphaltenes. Unlike single-color LDI MS, the mass spectra are shown here to be independent of the (A) surface mass density of asphaltenes, (B) time of ion acquisition, or (C and D) either laser power.^{33,34}

LIAD-EI-MS. Most probable asphaltene molecular weights are 750 Da, in excellent agreement with TRFD and other diffusion measurements.³⁸ Each method of molecular-weight determination has its own sensitivity profile; therefore, not all methods will yield exactly the same numbers. In addition, after the extensive difficulties uncovered in LDI regarding aggregation, it behooves experimentalists of any MS technique to establish the role of aggregation in mass spectral results.

The mass spectrometric method applied to asphaltenes that has had perhaps the greatest scrutiny is electrospray ionization Fourier transform ion cyclotron resonance mass spectroscopy (ESI-FT-ICR-MS).^{39–44} ESI is known to be

(29) Hortal, A. R.; Martínez-Haya, B.; Lobato, M. D.; Pedrosa, J. M.; Lago, S. On the determination of molecular weight distributions of asphaltenes and their aggregates in laser desorption ionization experiments. *J. Mass Spectrom.* **2006**, *41*, 960.

(30) Martínez-Haya, B.; Hortal, A. R.; Hurtado, P. M.; Lobato, M. D.; Pedrosa, J. M. Laser desorption/ionization determination of molecular weight distributions of polycyclic aromatic carbonaceous compounds and their aggregates. *J. Mass Spectrom.* **2007**, *42*, 701–713.

(31) Hortal, A. R.; Hurtado, P. M.; Martínez-Haya, B.; Mullins, O. C. Molecular weight distributions of coal and petroleum asphaltenes from laser desorption ionization experiments. *Energy Fuels* **2007**, *21*, 2863–2868.

(32) Hurtado, P.; Hortal, A. R.; Martínez-Haya, B. MALDI detection of carbonaceous compounds in ionic liquid matrices. *Rapid Commun. Mass Spectrom.* **2007**, *21*, 3161–3164.

(33) Pomerantz, A. E.; Hammond, M. R.; Morrow, A. L.; Mullins, O. C.; Zare, R. N. Two-step laser mass spectrometry of asphaltenes. *J. Am. Chem. Soc.* **2008**, *130* (23), 7216–7217.

(34) Pomerantz, A. E.; Hammond, M. R.; Morrow, A. L.; Mullins, O. C.; Zare, R. N. Asphaltene molecular weight distribution determined by two-step laser mass spectrometry. *Energy Fuels* **2009**, *23*, 1162–1168.

(35) Merdignac, I.; Desmazieres, B.; Terrier, P.; Delobel, A.; Laprevote, O. Analysis of raw and hydrotreated asphaltenes using off-line and on-line SEC/MS coupling. Proceedings of the Heavy Organic Deposition, Los Cabos, Baja California, Mexico, 2004.

(36) Cunico, R. I.; Sheu, E. Y.; Mullins, O. C. Molecular weight measurement of UG8 asphaltene by APCI mass spectroscopy. *Pet. Sci. Technol.* **2004**, *22*, 787.

(37) Qian, K.; Edwards, K. E.; Siskin, M.; Olmstead, W. N.; Mennito, A. S.; Dechert, G. J.; Hoosain, N. E. Desorption and ionization of heavy petroleum molecules and measurement of molecular weight distributions. *Energy Fuels* **2007**, *21*, 1042–1047.

(38) Pinkston, D. S.; Duan, P.; Gallardo, V. A.; Habicht, S. C.; Tan, X.; Qian, K.; Gray, M.; Muellen, K.; Kenttamaa, H. Analysis of asphaltenes and asphaltene model compounds by laser-induced acoustic desorption/Fourier transform ion cyclotron resonance mass spectrometry. *Energy Fuels* **2009**, *23*, 5564–5570.

(39) Rodgers, R. P.; Marshall, A. G. Petroleomics: Advanced characterization of petroleum derived materials by Fourier transform ion cyclotron resonance mass spectrometry (FT-ICR MS). In *Asphaltenes, Heavy Oils and Petroleomics*; Mullins, O. C., Sheu, E. Y., Hammami, A., Marshall, A. G., Eds.; Springer: New York, 2007; Chapter 3.

(40) Rodgers, R. P.; Schaub, T. M.; Marshall, A. G. Petroleomics: Mass spectrometry returns to its roots. *Anal. Chem.* **2005**, *77*, 20A–27A.

(41) Klein, G. C.; Kim, S.; Rodgers, R. P.; Marshall, A. G.; Yen, A.; Asomaning, S. Mass spectral analysis of asphaltenes. I. Compositional differences between pressure-drop and solvent-drop asphaltenes determined by electrospray ionization Fourier transform ion cyclotron resonance mass spectrometry. *Energy Fuels* **2006**, *20*, 1965–1972.

(42) Klein, G. C.; Kim, S.; Rodgers, R. P.; Marshall, A. G.; Yen, A. Mass spectral analysis of asphaltenes. II. Detailed compositional comparison of asphaltenes deposit to its crude oil counterpart for two geographically different crude oils by ESI FT-ICR MS. *Energy Fuels* **2006**, *20*, 1973–1979.

(43) Hughey, C. A.; Rodgers, R. P.; Marshall, A. G.; Qian, K.; Robbins, W. R. Identification of acidic NSO compounds in crude oils of different geochemical origins by negative ion electrospray Fourier transform ion cyclotron resonance mass spectrometry. *Org. Geochem.* **2002**, *33*, 743–759.

a very soft ionization method, not fragmenting covalent bonds and even enabling weakly bound di- or multimers to be measured.^{39–45} Moreover, molecular weights of asphaltenes measured by ESI–FT-ICR–MS do not come close to challenging the high-end mass capabilities.⁴⁵ Measured masses of a similar system to asphaltenes, carbon clusters, exceed 4000 Da and still do not come close to ESI–FT-ICR–MS limits.⁴⁶ Petroleum asphaltene molecular-weight distributions as measured by ESI–FT-ICR–MS are dominated by components in the 400–800 Da range.^{39–44} Moreover, the role of di- and multimers has clearly been delineated by ESI–FT-ICR–MS studies.³⁹ For example, Figure 8 shows the presence of dimers in the mass spectrum of a bitumen.³⁹ Again, without explicit accounting for aggregation, MS measurements on asphaltenes that yield much higher masses than the numerous studies cited above are likely to be suffering from aggregation effects.

Vapor Pressure Osmometry (VPO) and Size-Exclusion Chromatography (SEC). Figure 8 shows compelling evidence of asphaltene aggregation in the gas phase. Asphaltene aggregation has not only impeded proper use of LDI–MS in many laboratories but has also given rise to reports of excessive asphaltene molecular weights from VPO and SEC. This has been discussed in some length elsewhere,^{28,47} here, we summarize (and rely on upcoming sections 4 and 5). VPO determines the “molarity” of nonvolatile diluents in a volatile solvent of choice. This diluent acts as an impurity, lowering the solvent Gibbs free energy and thereby lowering the vapor pressure. When the measured vapor pressure reduction is related to the known mass addition, a molecular weight is obtained. Typically, VPO requires 1% or so addition of diluents to see a reasonable signal. However, VPO does not determine what is covalently linked but rather is sensitive to whatever aggregate species exist in solution. If aggregation changes with concentration, then concentration-dependent “molecular weights” are obtained; this is widely known for VPO applied to asphaltenes. As we shall see below, asphaltene nanoaggregates undergo cluster formation at $\sim 10^{-3}$ mass fraction in toluene and asphaltene molecules form nanoaggregates at 10^{-4} mass fraction. The insidious problem is this; VPO studies of asphaltenes have been able to approach dissociation of the clusters but not dissociation of the nanoaggregates.

Ideally, SEC separates according to molecular size. The SEC column packing material contains a distribution of pores; large species cannot fit into small pores and thus move through the column quickly. Smaller analytes access smaller

(44) McKenna, A. M.; Purcell, J. M.; Rodgers, R. P.; Marshall, A. G. Atmospheric pressure photoionization Fourier transform ion cyclotron resonance mass spectrometry for detailed compositional analysis of petroleum. Proceedings of the 9th International Conference on Petroleum Phase Behavior and Fouling, Victoria, British Columbia, Canada, June 15–19, 2008; Abstract 17.

(45) Fenn, J. B. 2002 Nobel Lecture: “Electrospray Wings for Molecular Elephants”, http://nobelprize.org/nobel_prizes/chemistry/laureates/2002/fenn-lecture.html.

(46) Purcell, J. M.; Hendrickson, C. L.; Dunk, P.; Kroto, H.; Marshall, A. G. Carbon cluster structural characterization by gas-phase ion–molecule reactions in an FT-ICR mass spectrometer. Proceedings of the 55th American Society for Mass Spectrometry Annual Conference on Mass Spectrometry, Indianapolis, IN, June 3–7, 2007; Poster MPD068.

(47) Mullins, O. C. Rebuttal to Comment by Professors Herod, Kandiyoti, and Bartle on “Molecular size and weight of asphaltene and asphaltene solubility fractions from coals, crude oils and bitumen” by S. Badre, C. C. Goncalves, K. Norinaga, G. Gustavson, and O. C. Mullins. *Fuel* 2007, 86, 309.

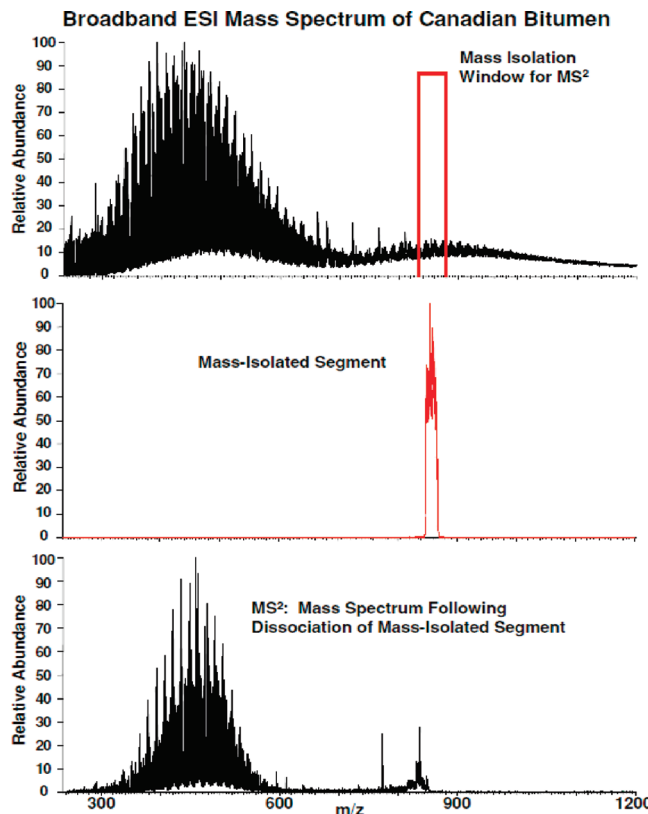


Figure 8. Low-resolution ESI mass spectrum of a Canadian bitumen (top) obtained at high analyte concentration (10 mg/mL), showing a clear bimodal distribution that suggests multimer formation.³⁹ Isolation of a mass segment (isolation window shown in the upper right) selects the mass segment shown in the middle panel. Subsequent gentle collision-induced dissociation (MS²) of the isolated species results in the regeneration of the same monomer species (bottom) previously observed in the broadband mass spectrum (top), strongly suggesting that the higher molecular-weight species are noncovalent multimers.³⁹

pores and move through the column with greater retention times. By calibration with known standards, SEC chromatograms are interpreted in terms of molecular weight. SEC applied to asphaltenes suffers many debilitating limitations in terms of absolute molecular-weight determination. A typical SEC standard is polystyrene, but asphaltenes are very different from polystyrene. Asphaltenes can interact with the column packing material, precluding proper correlations of retention time to molecular weight.⁴⁸ Typical SEC packing materials, polystyrene–divinyl benzene, do not survive use of toluene as a solvent; other solvents must be selected. Some groups have used *N*-methyl-2-pyrrolidone (NMP) as their solvent of choice, obtaining bimodal asphaltene molecular-weight distributions, with the larger peak being in the megadalton range.²⁷ However, NMP is known to flocculate up to $1/2$ of petroleum asphaltenes.^{13,28,49} The megadalton peak in the SEC chromatogram is likely the expected asphaltene flocs that occur when asphaltene is exposed to NMP. In addition, a comparison of NMP versus tetrahydrofuran (THF) gave significantly different

(48) Behrouzi, M.; Luckham, P. F. Limitations of size-exclusion chromatography in analyzing petroleum asphaltenes: A proof by atomic force microscopy. *Energy Fuels* 2008, 22, 1792–1798.

(49) Ascanius, B. E.; Garcia, D. M.; Andersen, S. I. Analysis of asphaltenes subfractionated by *N*-methyl-2-pyrrolidone. *Energy Fuels* 2004, 18, 1827.

SEC chromatograms probably because of differing and less asphaltene aggregation in THF (cf. ref 47). In any event, SEC is less than useful for asphaltene molecular-weight determination. Finally, as we shall see, the hierarchical state of asphaltene aggregation is very complex for a good asphaltene solvent, toluene. There is simply an unknown state of asphaltene aggregation in other not as good solvents in use for SEC. Because of these large numbers of reasons, SEC is not useful for absolute molecular-weight determination of asphaltenes but can still be used for very qualitative uses, for example, to establish trends. It must be understood that any observed trends in SEC with different asphaltene samples could be due to changes in molecular weight, aggregation, and/or adherence to the column packing.

3.2. Size of Asphaltene PAHs. Direct molecular imaging has provided valuable information regarding the size of asphaltene PAHs. Figure 9 shows a histogram of long axis dimensions of asphaltene PAHs as obtained by scanning tunneling microscopy (STM).⁵⁰ Individual asphaltene molecules were imagined with STM on different surfaces, and the PAH ring systems were resolved. These are difficult experiments; thus, the profile is not smooth, and a relatively small number of molecules were analyzed. Nevertheless, the trends are clear; the bulk of the PAHs have a long axis in the range around ~ 1 nm, which would correspond to roughly ~ 7 fused rings.⁵⁰

These imaging results were supported by high-resolution transmission electron microscopy (HRTEM). The aromatic sheets in petroleum asphaltenes were found to be ~ 1 nm, while for coal-derived asphaltenes, the PAH sheets are smaller, 0.7 nm.^{51,52} Analysis of the aromatic bands in the Raman spectra of asphaltenes yields the conclusion that the PAHs are roughly 8 fused rings.^{53,54} Similar conclusions were obtained from ¹³C NMR.⁵⁵ Recent measurements using ¹³C distortionless enhancement by polarization transfer (DEPT) methods obtained roughly 27 carbons per (petroleum) asphaltene aromatic cluster, corresponding to about 7 fused rings.⁵⁶ These ¹³C NMR results were shown to be largely consistent with FCS diffusion results.⁵⁶ In addition, the TRFD studies showed that model alkyl aromatics with 7 fused rings match most likely asphaltene rotational correlation times.^{9–15}

(50) Zajac, G. W.; Sethi, N. K.; Joseph, J. T. Molecular imaging of asphaltenes by scanning tunneling microscopy: Verification of structure from ¹³C and proton NMR data. *Scanning Microsc.* **1994**, *8*, 463.

(51) Sharma, A.; Groenzin, H.; Tomita, A.; Mullins, O. C. Probing order in asphaltenes and aromatic ring systems by HRTEM. *Energy Fuels* **2002**, *16*, 490.

(52) Sharma, A.; Mullins, O. C. Insights into molecular and aggregate structures of asphaltenes by HRTEM. In *Asphaltene, Heavy Oils and Petroleomics*; Mullins, O. C., Sheu, E. Y., Hammami, A., Marshall, A. G., Eds.; Springer: New York, 2007; Chapter 8.

(53) Bouhadda, Y.; Bormann, D.; Sheu, E. Y.; Bendedouch, D.; Krallafa, A.; Daoua, M. Characterization of Algerian Hassi-Messaoud asphaltene structure using Raman spectrometry and X-ray diffraction. *Fuel* **2007**, *86*, 1855–1864.

(54) Bouhadda, Y.; Fergoug, T.; Sheu, E. Y.; Bendedouch, D.; Krallafa, A.; Bormann, D.; Boubguira, A. Second order Raman spectra of Algerian Hassi-Messaoud asphaltene. *Fuel* **2008**, *87*, 3481–3482.

(55) Scotti, R.; Montanari, L. Molecular structure and intermolecular interaction of asphaltenes by FT-IR, NMR and EPR. In *Structures and Dynamics of Asphaltenes*; Mullins, O. C., Sheu, E. Y., Eds.; Plenum Press: New York, 2008; Chapter 3.

(56) Andrews, A. B.; Edwards, J.; Shih, W.-C.; Norinaga, K.; Mullins, O. C. Coal asphaltene molecular size by fluorescence correlation spectroscopy and ¹³C nuclear magnetic resonance. *Energy Fuels* **2010**, manuscript submitted.

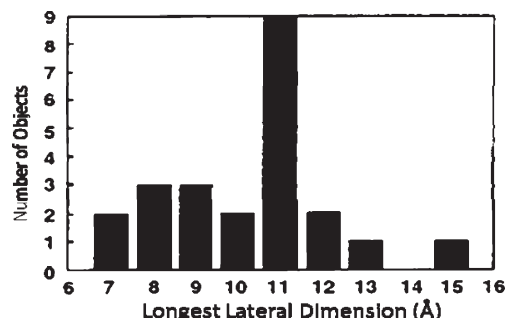


Figure 9. Histogram of the distribution of asphaltene PAH sizes by STM.⁵⁰ PAHs of ~ 7 fused aromatic rings are the most likely for asphaltenes.

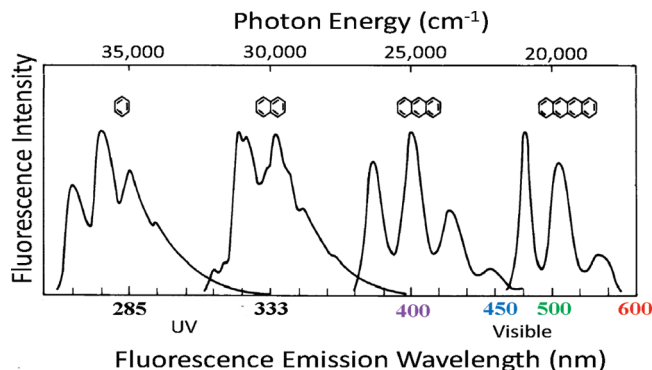


Figure 10. Fluorescence emission spectra of a series of linear PAHs (the acenes) exhibit a red shift with increasing numbers of fused rings.⁶⁴

Another method of testing PAH ring size distributions in asphaltenes is to probe their optical absorption and emission spectra. The enormous difference in appearance of (colorless) benzene and (black) graphite is due to their differences in electronic structure of isolated versus fused aromatic rings, validating such an approach. Moreover, there has never been any disagreement about the optical absorption spectra^{57–59} or fluorescence emission spectra of asphaltenes.⁶⁰ The ability to treat concentration effects,⁶⁰ quantum yields,¹⁷ fluorescence lifetimes,^{61–63} in addition to the spectral characteristics within a single framework for crude oils and asphaltenes⁶⁴ lends credence to the utility of spectral analysis.

To interpret asphaltene spectra, it is essential to establish the factors that govern the energy (thus, wavelength) of PAH absorption. One primary factor is related to basic quantum

(57) Mullins, O. C. Asphaltenes in crude oil: Absorbers and/or scatterers in the near-infrared. *Anal. Chem.* **1990**, *62*, 508.

(58) Mullins, O. C.; Zhu, Y. First observation of the Urbach tail in a multicomponent organic system. *Appl. Spectrosc.* **1992**, *46*, 354.

(59) Mullins, O. C.; Mitra-Kirtley, S.; Zhu, Y. Electronic absorption edge of petroleum. *Appl. Spectrosc.* **1992**, *46*, 1405.

(60) Downare, T. D.; Mullins, O. C. Visible and near-infrared fluorescence of crude oils. *Appl. Spectrosc.* **1995**, *49*, 754.

(61) Wang, X.; Mullins, O. C. Fluorescence lifetime studies of crude oils. *Appl. Spectrosc.* **1994**, *48*, 977.

(62) Owens, P.; Ryder, A. G.; Blamey, N. J. F. Frequency domain fluorescence lifetime study of crude petroleum oils. *J. Fluoresc.* **2008**, *18*, 997–1006.

(63) Ryder, A. G.; Przyjalgowski, M. A.; Feely, M.; Szczupak, B.; Glynn, T. J. Time-resolved fluorescence microspectroscopy for characterizing crude oils in bulk and hydrocarbon-bearing fluid inclusions. *Appl. Spectrosc.* **2004**, *58*, 1106.

(64) Mullins, O. C. Optical interrogation of aromatic moieties in crude oils and asphaltenes. In *Structures and Dynamics of Crude Oils*; Mullins, O. C., Sheu, E. Y., Eds.; Plenum Press: New York, 1998; Chapter 2.

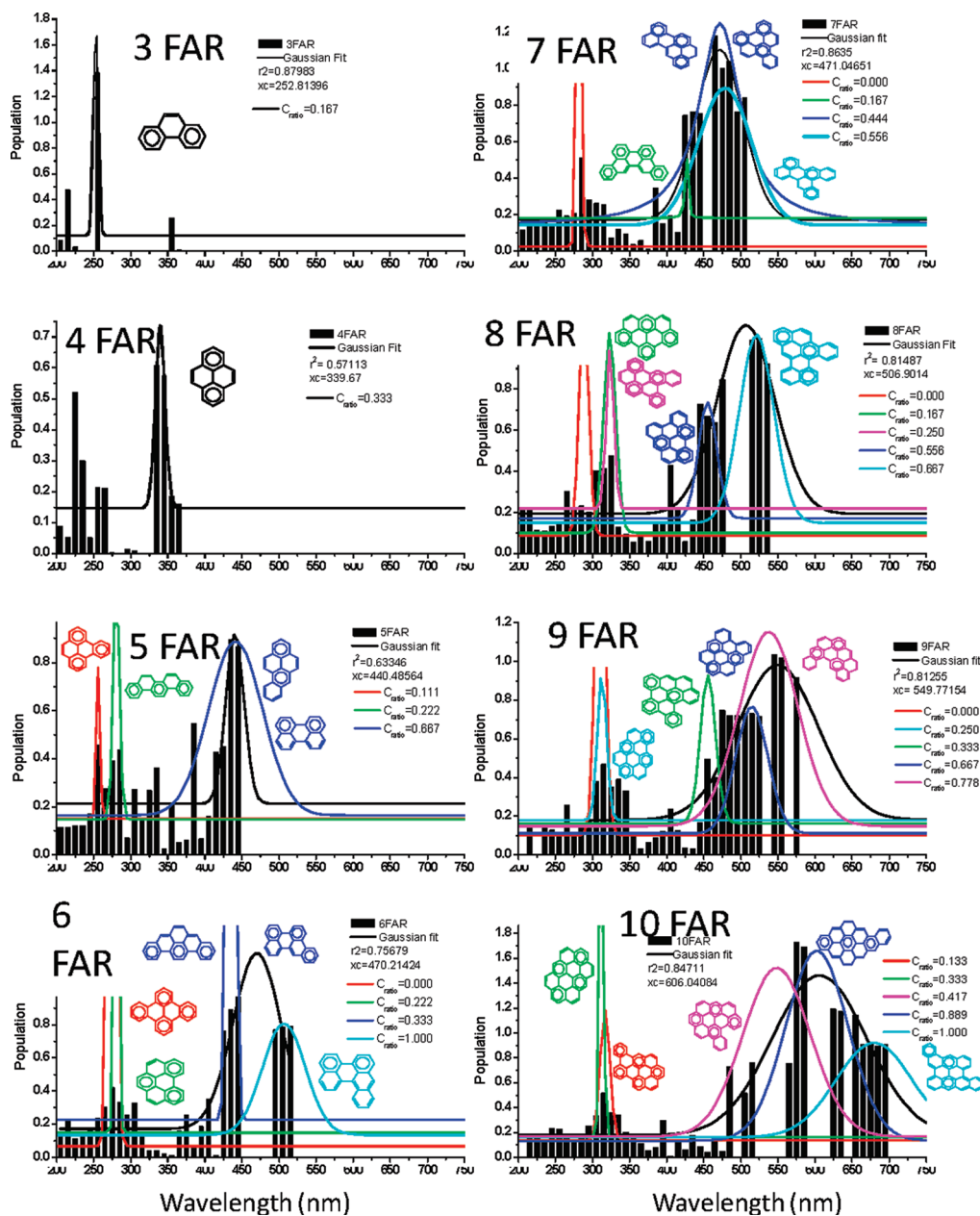


Figure 11. Molecular orbital theory predicting optical spectra (absorption and emission) applied to large numbers of candidate asphaltene PAHs.^{66–70}

mechanics. The transition energies of the π -electron wave functions are governed to a large degree by the size of the aromatic ring system in accordance with the well-known “quantum particle in a box”. Figure 10 depicts this for a linear arrangement of rings in different PAHs, the acenes.

A second factor that governs PAH spectral properties is the content of aromatic “sextet” carbon versus the isolated-double-bond carbon, with this language coming from the

Clar representation.^{65–70} This will be explained below. Here, we use the primary result; asphaltene PAHs are dominated by aromatic-sextet carbon and not isolated-double-bond carbon. This is in accordance with the greater stability of aromatic-sextet carbon. Moreover, it has previously been shown that crude oils and asphaltenes obey the Urbach tail formalism, which was initially developed in solid-state physics and which is predicated on systematic population distributions of electronic absorbers.^{58,59,64} Thus, using spectra to ferret out asphaltene PAH distributions is a sensible objective.

(65) Clar, E. *The Aromatic Sextet*; Wiley: London, U.K., 1972.

(66) Ruiz-Morales, Y. HOMO–LUMO gap as an index of molecular size and structure for polycyclic aromatic hydrocarbons (PAHs) and asphaltenes: A theoretical study. *J. Phys. Chem. A* **2002**, *106*, 11283.

(67) Ruiz-Morales, Y. Molecular orbital calculations and optical transitions of PAHs and asphaltenes. In *Asphaltene, Heavy Oils and Petroleomics*; Mullins, O. C., Sheu, E. Y., Hammami, A., Marshall, A. G., Eds.; Springer: New York, 2007; Chapter 4.

(68) Ruiz-Morales, Y.; Mullins, O. C. Polycyclic aromatic hydrocarbons of asphaltenes analyzed by molecular orbital calculations with optical spectroscopy. *Energy Fuels* **2007**, *21*, 256.

(69) Ruiz-Morales, Y.; Wu, X.; Mullins, O. C. Electronic absorption edge of crude oils and asphaltenes analyzed by molecular orbital calculations with optical spectroscopy. *Energy Fuels* **2007**, *21*, 944.

(70) Ruiz-Morales, Y.; Mullins, O. C. Simulated and measured optical absorption spectra of asphaltenes. *Energy Fuels* **2009**, *23*, 1169–1177.

Exhaustive molecular orbital calculations were performed on > 500 candidate asphaltene PAHs for the purpose of accounting for the measured optical properties of asphaltenes.^{66–70} Results from some of the PAHs with different numbers of fused aromatic rings (FARs) are shown in Figure 11. The red shift with increasing numbers of FARs is evident. Careful examination of structures in Figure 11 also shows increased red shifts associated with a greater fraction of isolated-double-bond carbon.

Using a presumed distribution of asphaltene PAHs given in Figure 12, a theoretical asphaltene absorption spectrum is obtained (cf. Figure 13).⁷⁰ The experimental and theoretical spectra closely match, as shown in Figure 13; thus, the PAH distribution in Figure 12 appears reasonable.

Each π electron has an oscillator strength of 1.⁷¹ Consequently, each π electron registers in the optical absorption spectrum; they cannot hide. If a π electron does not absorb in the near-infrared (NIR) or the visible, then it must absorb in the ultraviolet (UV). Thus, the PAH distribution in asphaltenes not only dictates the NIR and visible absorption but also the extent of increase in the UV absorption above the visible. Significantly different PAH distributions than that of Figure 12 do not reproduce the proper absorption spectrum for asphaltenes.⁷⁰

In the interpretation of electronic absorption spectra of asphaltenes, it is important to establish whether the absorption spectra are affected by aggregation, thus by concentration effects. Figure 14 establishes that there is no detectable effect of (nanocolloidal) aggregation on asphaltene absorption spectra. Indeed, there has been confusion about this point in the literature. That is, asphaltene spectra strictly obey the Beer–Lambert law; the absorption spectra do not exhibit any appreciable nonlinearities because of aggregation.

Figure 14 establishes that the optical absorption spectra of asphaltenes are independent of the concentration in the range of the CNAC and the clustering concentration (cf. sections 4 and 5).⁶⁹ Consequently, the absorption spectra are (incoherent) sums of the absorption spectra of the constituent asphaltene molecules without charge-transfer effects or other concentration-dependent electronic phenomena.⁶⁹ If the asphaltenes phase destabilize, forming flocs, then light scattering can become quite strong, contributing to the loss of transmitted light via optical light scattering (not changing optical absorption). Indeed, detection of light scattering is the preferred laboratory method to detect asphaltene phase destabilization.⁷²

In addition, the asphaltene PAH distribution presumed in Figure 12 can be used to predict the asphaltene fluorescence emission spectrum in Figure 15.⁷⁰ The theoretical fluorescence emission spectrum incorporates quantum yields from the energy gap law.¹⁷ Again, excellent agreement is obtained (the sharp line nature of the theoretical curve results because no solution line broadening is employed for the theoretical spectrum). The asphaltene PAH distribution in Figure 12 captures the major features of the actual asphaltene distribution.

We also note that there is very little fluorescence in asphaltenes from very small ring systems, e.g., naphthalene

(71) Hilborn, R. C. Einstein coefficients, cross sections, f values, dipole moments, and all that. *Am. J. Phys.* **1982**, *50*, 982.

(72) Hammami, A.; Ratulowski, J. Precipitation and deposition of asphaltenes in production systems: A flow assurance overview. In *Asphaltenes, Heavy Oils and Petroleomics*; Mullins, O. C., Sheu, E. Y., Hammami, A., Marshall, A. G., Eds.; Springer: New York, 2007; Chapter 23.

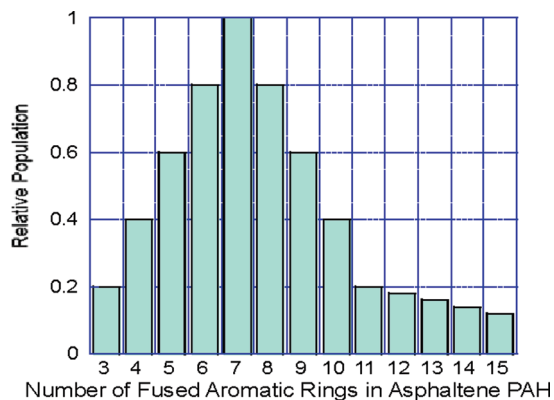


Figure 12. Presumed asphaltene PAH distribution used to calculate asphaltene optical absorption spectrum (Figure 13) and fluorescence emission spectrum (Figure 15). This PAH distribution is in accordance with measured molecular-weight distributions of asphaltenes provided that there is a single PAH per asphaltene molecule.

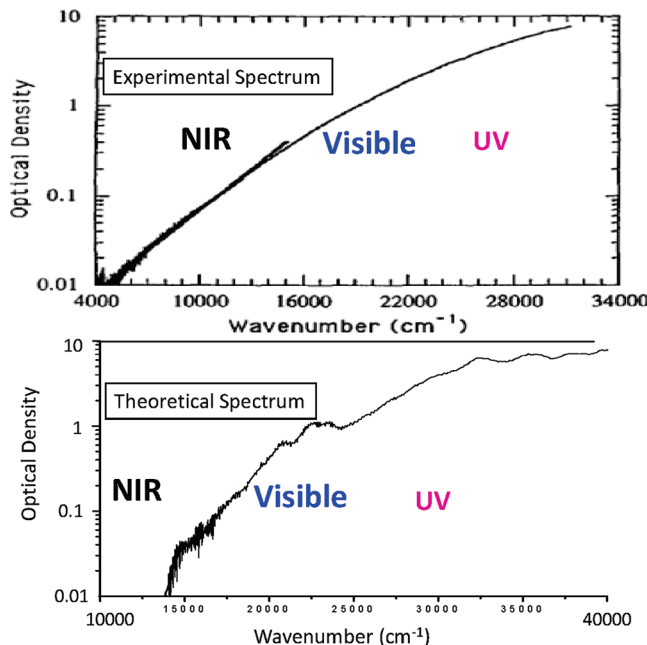


Figure 13. Experimental spectrum (top) and theoretical spectrum (bottom) for asphaltenes; the theoretical spectrum presumes the PAH distribution shown in Figure 12.⁷⁰ There is close agreement between the spectral location of the optical absorption and the magnitude of the increase in optical absorption in going from the near-infrared to the UV.

and anthracene. There are two possible reasons: (1) either these small ring systems are not present in quantity in asphaltenes, or (2) they are present; however, their electronic excitation is quenched by *intramolecular* nonradiative energy transfer. Quenching opens up a new decay channel for excited electronic states; thus, one signature of significant quenching is a reduction in fluorescence lifetimes.¹⁶ The intermolecular quenching effect on asphaltene and crude oil lifetimes is well-known at high concentrations.^{61–63} Fluorescence lifetimes of dilute solutions of asphaltenes were found to be comparable to those of dilute solutions of maltenes; no intramolecular quenching was detected.⁷³

(73) Ralston, C. Y.; Mitra-Kirtley, S.; Mullins, O. C. Small population of one to three fused-ring aromatic molecules in asphaltenes. *Energy Fuels* **1996**, *10*, 623.

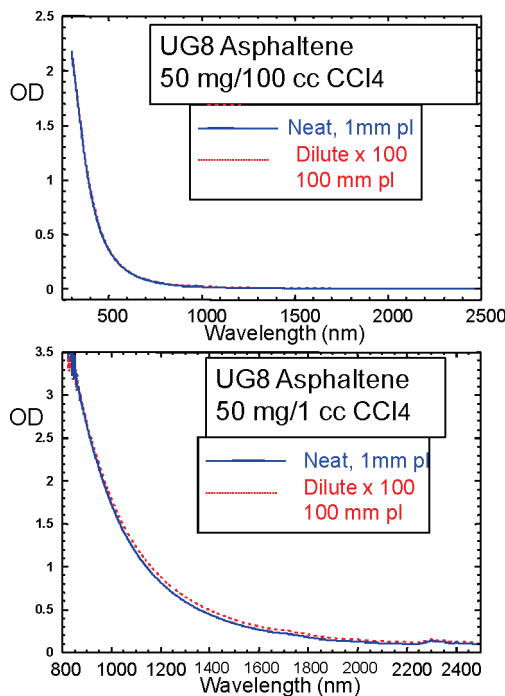


Figure 14. Optical absorption spectra of asphaltenes versus concentration. (Top) Spectrum for 0.5 g/L solution for 1 mm path length (pl) overlays the spectrum for 0.005 g/L solution for 100 mm pl. (Bottom) Spectrum for 50 g/L for 1 mm pl overlays the spectrum for 0.5 g/L for 100 mm pl (subtle differences are attributed to beam walkoff in the 100 mm cell). The dilute and concentrated solutions exhibit their absorption edge at the visible and NIR spectra, respectively. There is no nonlinearity in the absorption spectrum of asphaltenes throughout the visible and NIR spectra range.

Thus, the low intensity of fluorescence from smaller ring systems in asphaltenes is ascribed to the small fraction of small PAHs in asphaltenes.⁷³ In addition, perylene, a 5-ring PAH has been found to dominate the fluorescence of two light crude oils.⁷⁴ Finding a 5-ring PAH in a light crude oil is consistent with finding much larger PAHs in asphaltenes. These results are in accordance with very recent asphaltene spectra, showing no peaks from single aromatic rings in asphaltene spectra (cf. section 6.1).

3.3. Type of Asphaltene PAHs. There has been a long-standing discussion in the asphaltene literature about the type of PAHs in asphaltenes. This discussion revolved around pericondensation (with 3 rings sharing a bridgehead) versus catacondensation (with 2 rings sharing a side). This discussion was changed dramatically for asphaltenes^{66–70} with the incorporation of the Clar representation of PAHs.⁶⁵ In this representation, no 2 adjacent, fused aromatic rings can both be sextets; that is, no two adjacent hexagons can both “have circles”. Figure 16 shows naphthalene in the Clar representation. These representations reflect electron density and bond order. The top of Figure 16 shows essentially equivalent representations, with the aromatic-sextet ring on the left side of naphthalene. The bottom of Figure 16 shows the two Kekulé structures, each within the Clar representation, which together yield the symmetric naphthalene. The CC naphthalene bond lengths are not all equal, and the ordering is given by the Clar representations.

(74) Juyal, P.; McKenna, A.; Andrews, A. B.; Chen, A.; Mullins, O. C.; Rodgers, R. P.; Marshall, A. G. The origin of the blue coloration of a condensate. Manuscript in preparation.

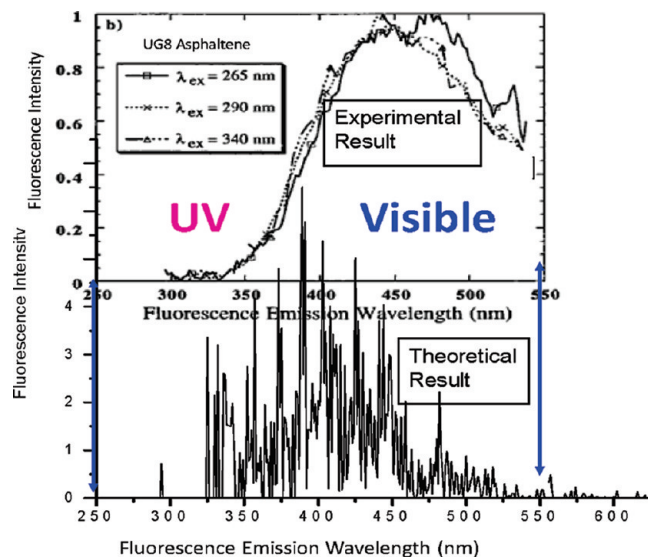


Figure 15. Experimental and theoretical fluorescence emission spectra of asphaltenes.⁷⁰ The theoretical curve does not incorporate line broadening that naturally occurs in solution and is found in the experimental spectrum. The close agreement validates the presumed asphaltene PAH distribution shown in Figure 12.

Pure sextet compounds, such as benzene, triphenylene, and hexabenzocoronene, are very stable and have blue-shifted spectra. When PAHs have increasing fractions of isolated-double-bond carbon, they become less stable and have red-shifted optical absorption spectra.^{65–70} The question arises what type of carbon is found in asphaltenes; aromatic-sextet or isolated-double-bond carbon. The stability of sextet carbon provides a clue; asphaltenes are stable for geologic time. To solve this question for asphaltenes, one must revert to X-ray spectroscopy.

X-ray spectroscopy has been very useful to probe electronic structure. Instead of relying on valence shell transitions of optical spectroscopy, X-ray spectroscopy relies on exciting empty valence orbitals from inner electron shells.⁷⁵ Often there are large peak shifts associated with a different chemical identity of compounds. For example, different sulfur compounds from sulfide to sulfate exhibit a ~10 eV shift of the 1s–3p transition in accordance with the formal oxidation state of sulfur.⁷⁶ Consequently, sulfur X-ray spectroscopy is very useful for analysis of sulfur in asphaltenes as will be described.^{76,77} Similarly, chemical speciation of asphaltene nitrogen has been analyzed on the basis of peak energy differences for different nitrogen chemical functions, such as pyridinic and pyrrolic nitrogen, which exhibit large 1s–π* peak differences.⁷⁸ Naturally, the question arises whether X-ray spectroscopy can be useful for carbon in asphaltenes.

(75) Stohr, J. *NEXAFS Spectroscopy*; Springer-Verlag: Berlin, Germany, 1992.

(76) George, G. N.; Gorbaty, M. L. Sulfur K-edge X-ray absorption spectroscopy of petroleum asphaltenes. *J. Am. Chem. Soc.* **1989**, *111*, 3182.

(77) Mitra-Kirtley, S.; Mullins, O. C. Sulfur chemical moieties in carbonaceous materials. In *Asphaltene, Heavy Oils and Petroleomics*; Mullins, O. C., Sheu, E. Y., Hammami, A., Marshall, A. G., Eds.; Springer: New York, 2007; Chapter 6.

(78) Mitra-Kirtley, S.; Mullins, O. C.; Chen, J.; van Elp, J.; George, S. J.; Cramer, S. P. Determination of the nitrogen chemical structures in petroleum asphaltenes using XANES spectroscopy. *J. Am. Chem. Soc.* **1993**, *115*, 252.

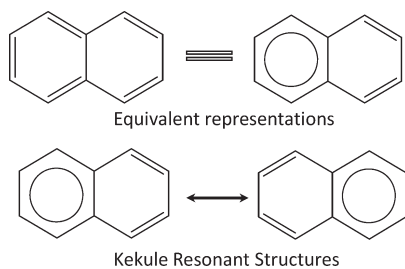


Figure 16. (Top) Two essentially equivalent representations of naphthalene with one aromatic-sextet ring (the left ring in both top structures depicted) and two isolated double bonds in the “right ring” within the Clar representation.⁶⁵ (Bottom) Two corresponding Kekulé resonant structures contribute to naphthalene, making it symmetric.

Standard absorption X-ray spectroscopy in asphaltenes for carbon analysis is somewhat problematic ironically because of the high concentration of carbon in asphaltenes. Nonlinear effects can result from too much absorption of carbon X-ray bands. In addition, the very low energy of the carbon K-edge X-ray (285 eV) gives rise to very short penetration lengths; thus, sample surface effects can dominate, as opposed to bulk analysis, depending upon detection methods. Consequently, carbon X-ray Raman spectroscopy (XRRS) is most appropriate for analysis of asphaltene carbon.^{79–81} In XRRS, high-energy X-rays are inelastically scattered, leaving the scatterer (here, carbon atoms) in electronically excited states.^{79–81} The X-ray spectrum is obtained using a small-bandwidth X-ray source (synchrotron) and dispersing the scattered X-rays.

The simple idea is that if a PAH is pure aromatic-sextet carbon, the $1s-\pi^*$ X-ray absorption line (as determined by XRRS) will be narrow. The isolated-double-bond carbon has a slightly different $1s-\pi^*$ line position; thus, for compounds with increasing amounts of isolated-double-bond carbon, the $1s-\pi^*$ line width for the PAH will increase. Figure 17 shows that the Clar description of PAHs matches the $1s-\pi^*$ line width, as measured by XRRS for a large number of PAHs. Compounds with greater aromatic-sextet carbon have smaller line widths. The measured asphaltene line width is ~ 1.4 eV; not surprisingly, asphaltenes are dominated by aromatic-sextet carbon. For years, the discussion regarding asphaltene carbon has been whether it is pericondensed versus catacondensed without explanation why it should be either. We now see this discussion was misplaced. Asphaltene carbon is primarily aromatic-sextet carbon because this carbon is more stable. Many pericondensed structures have substantial sextet carbon (cf. Figure 11). Nevertheless, triphenylene is catacondensed yet pure sextet carbon.

3.4. Number of PAHs per Asphaltene Molecule. The number of distinct PAHs (not conjugated) in a single asphaltene molecule is difficult to address, thereby allowing divergent conjectures. Some proposals incorporated many different isolated PAHs within a molecule and acquired the sobriquet

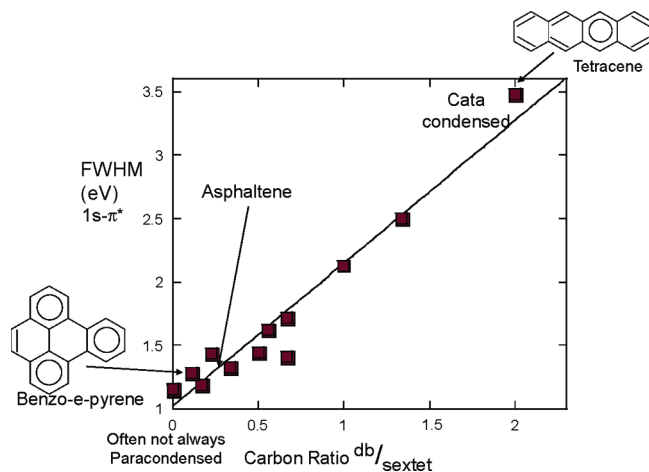


Figure 17. $1s-\pi^*$ line width as determined by XRRS versus the ratio of isolated-double-bond carbon to aromatic-sextet carbon.^{80,81} Sextet carbon but not isolated-double-bond carbon dominates asphaltene aromatics. Sextet carbon is known to be more stable and often predominates in pericondensed ring systems.^{65,66}

“archipelago model”, with the islands being the individual covalently cross-linked PAHs. These models were based on bulk decomposition studies. Indeed, the less than optimal method to determine the architecture of a house is to burn it down and sift through the ashes. Decomposition data are easy to misinterpret unless it is performed under very controlled conditions. Fortunately, there is increasing consistency between nondestructive methods and carefully controlled destructive methods for the determination of the number of PAHs per asphaltene molecule.

More recent data indicates that the predominant asphaltene molecular architecture has a single PAH; this has been termed “like your hand” or “island” model. When it was believed that asphaltene molecular weights were quite high, there was little constraint on the proposed number of PAHs in each molecule. However, it is now known that asphaltene molecular weights are relatively small. Moreover, the distribution of asphaltene PAHs is centered roughly at 7 fused rings and, thus, not small. The combination of small mass and intermediate-sized PAHs means that not many PAHs will fit into the molecular-weight limit. For example, a 7-membered fused ring system with the appropriate alkyl carbon fraction and a sulfur atom weighs ~ 750 Da. Indeed, some proponents of the archipelago model are reduced to models with two PAH islands. Geographers will have to decide if this constitutes an archipelago (e.g., the United Kingdom archipelago); we will examine studies addressing this issue.

For 10 years, the only studies that strongly supported the island model were the TRFD molecular diffusion studies.^{9–15} We show in pictorial fashion what would be expected for TRFD data for the two molecular model types, island versus archipelago (Figure 18). The plots are color-coded; small PAHs (small number of fused rings) are blue fluorescence emitters, while big PAHs are red fluorescence emitters (cf. Figure 11). The island model is consistent with (1) small rotational correlation times for all asphaltenes and (2) large differences of correlation times between blue- and red-emitting PAHs. The archipelago model is consistent with large rotational correlation times. In addition, because the blue and red fluorophores are cross-linked, they undergo rotational diffusion with similar correlation times.

(79) Bergmann, U.; Mullins, O. C.; Cramer, S. P. Carbon Raman X-ray spectroscopy of asphaltenes. *Anal. Chem.* **2000**, *72*, 2609.

(80) Bergmann, U.; Groenzin, H.; Mullins, O. C.; Glatzel, P.; Fetzer, J.; Cramer, S. P. Carbon K-edge X-ray Raman spectroscopy supports simple yet powerful description of aromatic hydrocarbons and asphaltenes. *Chem. Phys. Lett.* **2003**, *369*, 184.

(81) Bergmann, U.; Mullins, O. C. Carbon X-ray Raman spectroscopy of PAHs and asphaltenes. In *Asphaltenes, Heavy Oils and Petroleomics*; Mullins, O. C., Sheu, E. Y., Hammami, A., Marshall, A. G., Eds.; Springer: New York, 2007; Chapter 5.

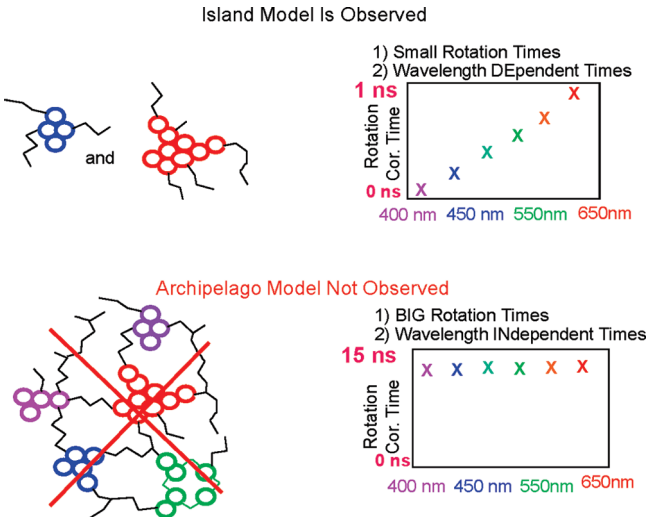


Figure 18. Color-coded pictorial representation of what the TRFD data should look like for the island versus archipelago molecular architecture for asphaltenes. All measured TRFD data on asphaltenes support the predominance of the “island molecular architecture” for asphaltenes with a single PAH per asphaltene molecule.¹⁵

Figure 19 provides compelling data that the island model dominates asphaltenes.^{9–15} Of course, these data do not rule out some contribution of asphaltene molecules with 2 or 0 PAHs for that matter. The possibility of interference of complexities in the TRFD data from energy transfer was checked; no telltale trace on fluorescence lifetimes by energy transfer was found.⁷³ In addition, the measured initial anisotropy in the TRFD experiments was near the theoretical limits.^{9–15} It is well-known that energy-transfer processes destroy polarization. The fact that large anisotropy was measured indicates that energy-transfer processes were not significant in these experiments. Many consistency checks were performed, including understanding the large molecular difference between coal-derived versus petroleum asphaltenes. In addition, the TRFD studies measured the same rotational diffusion of the porphyrins as a very different technique, perturbed angular correlation of γ -rays.⁸²

Recently, gas-phase, unimolecular decomposition (or equivalently collisionally induced dissociation) studies have been carried out by the Marshall group at Florida State University.^{83,84} The decomposition is not performed in the condensed phase but rather the gas phase, precluding intermolecular interactions or intermolecular chemical reactions during decomposition. In addition, a well-controlled molecular weight slice of the asphaltene gas-phase ions is selected for fragmentation. Different molecular weights and chemical classes are individually interrogated. An ensemble of isolated, ionized asphaltene molecules is subject to radio frequency, which causes the molecular ions to move with the field. This is performed in a helium bath, causing controllable

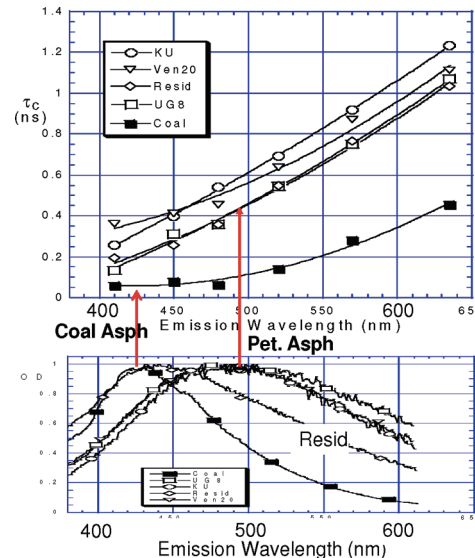


Figure 19. TRFD data for three virgin crude oil asphaltenes (KU, Ven20, and UG8), one petroleum resid asphaltene, and one coal-derived asphaltene. The TRFD data show (1) small rotational correlation times and (2) a large difference between correlation times for blue- versus red-emitting PAHs. The island model of asphaltene molecular architecture is supported.^{9–15}

collisions. Of course, for collision with helium, there is no interference by chemical reaction. The daughter products from this collision are then analyzed and compared to the parent.^{83,84}

The unimolecular decomposition data are striking. The original population of asphaltenes corresponds to the high-magnitude region inside the rectangle in Figure 20. The process of fragmentation yields daughter compounds that are displaced to the left (as shown by the red arrows labeled fragmentation). Molecular fragmentation results in the loss of the carbon number but not the loss of DBE (in other words, aromaticity)^{83,84} (DBE is “double bond equivalent” and equals the number of rings plus double bonds in the compound). However, studies of model compounds show that archipelago-type models (with two PAHs linked by an alkane linkage) are readily fragmented with the loss of both the carbon number and aromaticity. The data shown in Figure 20 apply to the basic nitrogen class of asphaltenes with a carbon number of ~45.^{83,84} Other carbon numbers and other chemical classes have given very similar results.^{83,84} These studies clearly support the island model as the predominant asphaltene molecular architecture. Moreover, conclusions from these well-controlled destructive studies are much more robust than uncontrolled pyrolysis of bulk asphaltene samples; the latter uncontrolled decomposition studies are the primary studies that were interpreted to support the archipelago model for asphaltenes. Because well-controlled destructive studies support the island molecular model for asphaltenes, the support for the archipelago model is greatly reduced.

Coal-Derived versus Petroleum Asphaltenes. Asphaltenes are a solubility classification; a toluene-soluble, *n*-heptane-insoluble classification is typically used. For petroleum, toluene solubility captures the heaviest aromatic fraction. However, for vacuum resid or coal-derived asphaltenes, toluene solubility does not capture the most aromatic component; therefore, the concept of asphaltenes for materials other than crude oils loses some significance. Nevertheless,

(82) Mullins, O. C.; Kaplan, M. Perturbed angular correlation studies of indium metalloporphyrin complexes. *J. Chem. Phys.* **1983**, *79*, 4475.

(83) McKenna, A. M.; Purcell, J. M.; Rodgers, R. P.; Marshall, A. G. Atmospheric pressure photoionization Fourier transform ion cyclotron resonance mass spectrometry for detailed compositional analysis of petroleum. Proceedings of the 9th International Conference on Petroleum Phase Behavior and Fouling, Victoria, British Columbia, Canada, June 15–19, 2008; Abstract 17.

(84) McKenna, A. M.; Purcell, J. M.; Rodgers, R. P.; Marshall, A. G. Petrophase 10th International Conference on Petroleum Phase Behavior and Fouling, Rio de Janeiro, Brazil, 2009.

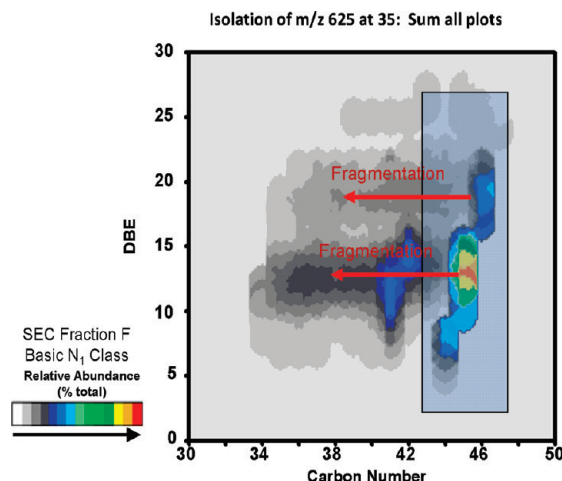


Figure 20. Gas-phase, unimolecular decomposition of asphaltene molecules via collision with helium gas. Fragmentation causes the loss of the carbon number but *not* a reduction of aromaticity. These data are consistent only with the island molecular architecture and not the archipelago.^{33,84}

these other types of asphaltenes are useful to understand and test concepts governing asphaltene chemical identity. Coal-derived asphaltenes provide a very interesting test platform. We consider asphaltenes obtained from the following process: first, coal was liquefied in a hydrogenation process according to published procedures.^{85,86} The coal liquids were then vacuum-distilled, giving rise to a resid. From the resid, a toluene-soluble, *n*-hexane-insoluble fraction was obtained. Coal-derived asphaltenes have been analyzed for several coals, and always one primary observation stands out; the coal-derived asphaltenes are approximately half the molecular weight of the virgin petroleum asphaltenes. This result has been obtained by the diffusion measurements TRFD^{11,13–15} and FCS^{22,23,56} and the MS methods LDI-MS³¹ and two-step laser ionization mass spectroscopy (L2MS).³⁴ For example, Figure 21 shows the L2MS data for a typical petroleum and coal-derived asphaltene.³⁴

The data in Figure 21 match the TRFD data presented in Figure 19; the coal-derived asphaltenes are half the molecular weight of the petroleum asphaltenes. Why? First, the coal-derived asphaltenes lack alkane because coals are alkane-deficient (thus, solid) compared to crude oil. In addition, these coal-derived asphaltenes are from a resid and, therefore, have lost alkane in the refining process.¹³ C NMR has been most useful to show that the carbon of coal-derived asphaltenes is ~82% aromatic, while for petroleum asphaltenes, it is ~50%.^{11,56} This alkane difference accounts for a big fraction of the mass difference but not all. The rest of the difference is seen in Figure 19. The coal asphaltene has a blue-shifted fluorescence emission spectrum¹¹ and a blue-shifted optical absorption spectrum;³¹ the coal-derived asphaltenes have smaller PAHs than the petroleum asphaltenes.

In addition, this is just freshman chemistry. The asphaltenes, whether from coal or crude oil, are a solubility classification; repulsive and attractive forces must balance. With the reduction of the repulsive alkane, the coal-derived

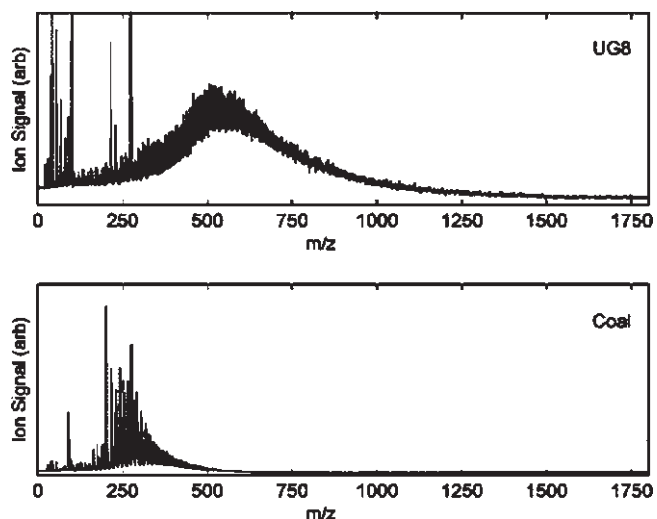


Figure 21. L2MS compares (bottom) a coal-derived asphaltene versus (top) a virgin crude oil asphaltene. All measurements of asphaltene molecular weight show the coal-derived asphaltenes are $\sim 1/2$ the mass of the petroleum asphaltenes.³⁴

asphaltenes must have smaller attractive forces and, thus, smaller PAHs. If this is true, then as a petroleum resid feedstock undergoes increasing catalytic hydrothermal cracking, the asphaltene molecules must become smaller with blue-shifted fluorescence; this has indeed been observed in a series of increasingly processed resid samples.¹⁴ Indeed, the resid fluorescence is seen to be blue-shifted in Figure 19.¹¹ Similar observations on asphaltenes have been made with regard to catalytic hydrogenation of a resid feedstock with an ebullated bed reactor.⁸⁷ As conversion proceeds, the alkanes are cracked off the predominantly single PAH and solubility decreases. That which was asphaltene becomes coke, and that which was resin becomes asphaltene, etc. With increasing conversion, the asphaltene PAHs become smaller.

Figure 22 shows proposed coal-derived and crude oil asphaltenes, illustrating the difference in molecular size, alkane content, and PAH size.

The observations that coal-derived asphaltenes are $1/2$ the size of virgin petroleum asphaltenes and that the reduction of alkane carbon causes the corresponding PAH to be smaller than petroleum makes sense *only if there is one PAH per asphaltene molecule*. If there were multiple PAHs per molecule (archipelago model), then a reduction of repulsion from the loss of alkane could be balanced by less attraction from a reduction in the *number* of PAHs. Consequently, there would be no connection between the alkane content and PAH size contrary to observation. In addition, the coal-derived asphaltenes have very little alkane carbon; therefore, it is difficult to propose archipelago models for coal-derived asphaltenes. There is little alkane carbon to intervene.

Fused Naphthenic Rings in Petroleum Asphaltenes. The petroleum asphaltenes depicted here are shown to have an attached cyclic alkane in accordance with the large hydrogen-donor activity of asphaltenes beyond that of alkyl aromatics.^{88,89} That is, compounds such as tetralin

(85) Hirano, K. Outline of NEDOL coal liquefaction process development (pilot plant program). *Fuel Process. Technol.* **2000**, 62 (2–3), 109–118.

(86) Ikeda, K.; Sakawaki, K.; Nogami, Y.; Inokuchi, K.; Imada, K. Kinetic evaluation of progress in coal liquefaction in the 1t/d PSU for the NEDOL process. *Fuel* **2000**, 79 (3–4), 373–378.

(87) Merdignac, I.; Quoineaud, A.-A.; Gauthier, T. Evolution of asphaltene structure during hydroconversion conditions. *Energy Fuels* **2006**, 20, 2028–2036.

(88) Gould, K. A.; Wiehe, I. A. Natural hydrogen donors in petroleum resids. *Energy Fuels* **2007**, 21, 1199–1204.

(89) Wiehe, I. A. *Process Chemistry of Petroleum Macromolecules*; CRC Press: Boca Raton, FL, 2008.

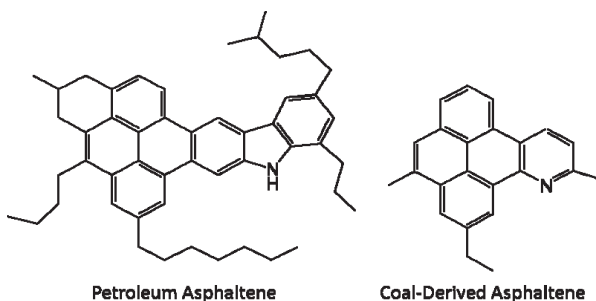


Figure 22. Proposed molecular structures for coal-derived versus petroleum asphaltenes accounting for known significant differences in terms of molecular weight, alkane composition, and PAH size.¹⁵

exhibit significant hydrogen-donor capability. Because asphaltenes likewise exhibit a high degree of hydrogen-donor capability,^{88,89} the corresponding analysis concludes that asphaltenes possess a significant fraction of naphthenic rings fused to aromatic moieties in asphaltenes. Initial ruthenium-ion-catalyzed oxidation (RICO) analyses were interpreted to yield large archipelago molecules for asphaltenes.⁹⁰ Subsequent work showed that these studies were limited because of inappropriate reaction temperatures, among other issues.⁹¹ Moreover, much of the interpretation of the RICO data is consistent with substantial fractions of fused naphthenic rings as opposed to aliphatics cross-linking separate PAHs.⁹² Other concerns have been raised with regard to the conclusions of the original RICO studies.⁹³ Naphthenic rings fused to aromatic rings are evidently an important component of asphaltenes.^{88,89}

Dissolved Organic Matter and Asphaltene Derivatives. An interesting extension of asphaltene science is in the realm of oceanography. The world's oceans have substantial quantities of dissolved organic matter (DOM) at the level of 10–100 gigatons.^{94–96} To put this into perspective, the total mass of atmospheric CO₂ is ~700 gigatons. The heaviest of the DOM is thought to be a derivative of asphaltenes and has roughly 7 fused aromatic ring PAHs.^{94–96} Figure 23 shows the ESI–FT-ICR–MS analysis of the ocean DOM.

The similarities between the DOM molecular structures and the asphaltene molecular structures are striking. The DOM has lost most alkane carbon and acquired carboxylic acid functionality, and not much has happened to the PAHs; perhaps these modifications are from bioactivity.^{94–96} Similar to the coal-derived asphaltenes, there is less debate regarding whether the DOM has fused ring systems because there is so little alkane carbon to possibly intervene.

4. Primary Aggregation: Asphaltene Nanoaggregates

4.1. Asphaltene Nanoaggregates.

Asphaltenes have a strong tendency to aggregate, and indeed, this impacts if not defines

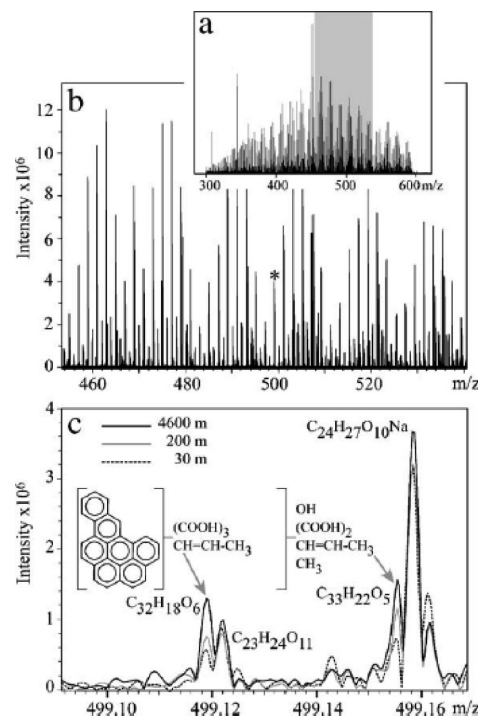


Figure 23. ESI–FT-ICR–MS spectra of marine dissolved organic matter samples from Antarctica at three water depths, 30, 200, and 4600 m.⁹⁶ (a) the complete spectrum (300–600 Da), (b) an enlarged spectral region, and (c) a very narrow mass range. Proposed structures are embedded. Because there is so little alkane carbon, preferred structures contain large fused ring systems⁹⁶ (the Clar representation was not used for the embedded structure in ref 96).

many of the physical characteristics of asphaltenes. The details of the aggregation process have been somewhat difficult to unravel in part because the primary aggregates have very small aggregation numbers. In addition, there is also a secondary aggregation process that has small aggregation numbers at least at times. Nevertheless, a large number of techniques have been used to investigate asphaltene aggregation and have provided consistent results, helping to achieve robust findings.

In addition to X-ray diffraction,⁹⁷ small-angle X-ray scattering (SAXS) and small-angle neutron scattering (SANS) have been employed by many workers and have been very useful in the characterization of colloidal asphaltene structures.^{98–106} Most of the studies agree on a colloidal view of asphaltene aggregates with characteristic sizes of 3–10 nm, depending

(90) Strausz, O. P.; Mojelsky, T. W.; Lown, E. M. The molecular structure of asphaltene: An unfolding story. *Fuel* **1992**, *71*, 1355.

(91) Artok, L.; Murata, S.; Nomura, M.; Satoh, T. Reexamination of the RICO method. *Energy Fuels* **1998**, *12*, 391–398.

(92) Su, Y.; Artok, L.; Murata, S.; Nomura, M. Structural analysis of the asphaltene fraction of an Arabian mixture by a ruthenium-ion-catalyzed oxidation reaction. *Energy Fuels* **1998**, *12*, 1265–1271.

(93) Mullins, O. C. Rebuttal of Strausz et al. regarding time resolved fluorescence depolarization. *Energy Fuels* **2009**, *23*, 2845–2854.

(94) Dittmar, T. The molecular level determination of black carbon in marine dissolved organic matter. *Org. Geochem.* **2008**, *39*, 396–407.

(95) Koch, B. P.; Dittmar, T. From mass to structure: An aromaticity index for high-resolution mass data of natural organic matter. *Rapid Commun. Mass Spectrom.* **2006**, *20*, 926–932.

(96) Dittmar, T.; Koch, B. P. Thermogenic organic matter dissolved in the abyssal ocean. *Mar. Chem.* **2006**, *102*, 208–217.

(97) Yen, T. F.; Erdman, J. G.; Pollack, S. S. Investigation of the structure of petroleum asphaltenes by X-ray diffraction. *Anal. Chem.* **1961**, *33* (11), 1587–1594.

(98) Sheu, E. Y. Colloidal properties of asphaltenes in organic solvents. In *Asphaltenes—Fundamentals and Applications*; Sheu, E. Y., Mullins, O. C., Eds.; Plenum Press: New York, 1995; Chapter 1.

(99) Sheu, E. Y. Petroleum and characterization of asphaltene aggregates using small angle scattering. In *Asphaltene, Heavy Oils and Petroleomics*; Mullins, O. C., Sheu, E. Y., Hammami, A., Marshall, A. G., Eds.; Springer: New York, 2007; Chapter 14.

(100) Wiehe, I. A.; Liang, K. S. Asphaltenes, resins, and other petroleum macromolecules. *Fluid Phase Equilib.* **1996**, *117*, 201–210.

(101) Barre, L.; Simon, S.; Palermo, T. Solution properties of asphaltenes. *Langmuir* **2008**, *24* (8), 3709–3717.

(102) Fenistein, D.; Barre, L. Experimental measurement of the mass distribution of petroleum asphaltene aggregates using ultracentrifugation and small-angle X-ray scattering. *Fuel* **2001**, *80* (2), 283–287.

(103) Fenistein, D.; Barre, L.; Espinat, D.; Livet, A.; Roux, J.-N.; Scarella, M. M. Viscosimetric and neutron scattering study of asphaltene aggregates in mixed toluene/heptane solvents. *Langmuir* **1998**, *14*, 1013–1020.

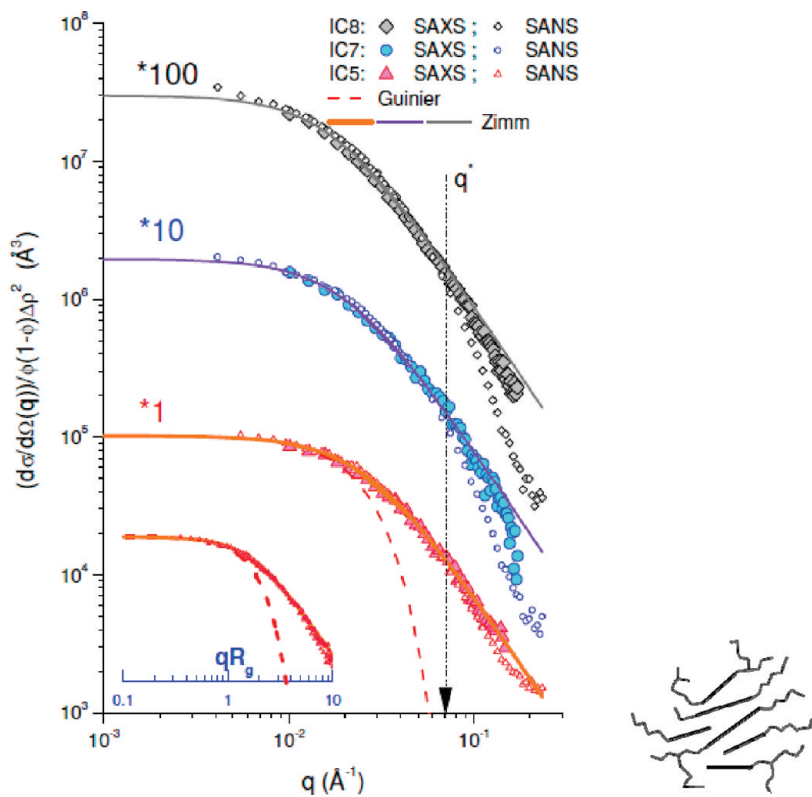


Figure 24. (Left) Comparison of SAXS and SANS spectra: variations of $I(q)/\phi\Delta\rho^2$ as a function of the wave-scattering vector q for solutions of different asphaltenes in toluene. The dotted and full lines represent, respectively, the Guinier and Zimm approximations in the small q domain.¹⁰⁶ The contrast of SAXS sensitivity to electron density, thus, the PAH stack, versus the SANS sensitivity to hydrogen, thus, the peripheral alkanes, gives the length scale of the interior PAH stack of the nanoaggregate, $\sim 14 \text{ \AA}$.¹⁰⁶ (Right) Proposed asphaltene nanoaggregate.

upon the asphaltene and solvent nature and thermodynamic conditions. Different studies find different geometries of colloidal particles, likely pointing to the non-unique geometric interpretation of the data. Recent work contrasting SAXS and SANS data has given insight into specific nanoaggregate structures.

We quote from ref 106: “Neutron and X-ray scattering experiments measure the scattered intensity $I(q)$, which probes the correlations between asphaltene-rich regions at a scale of the order of q^{-1} . The scattering vector q , defined as $q = 4\pi \sin \theta/\lambda$, where 2θ is the deviation angle and λ is the incident wavelength, acts as an inverse length scale. If SAXS and SANS offer a typical q range very similar (see Figure 24), they differ above all by the beam/matter interaction nature. X-rays interact with electrons, whereas neutrons interact with nuclei. The relevant characteristics of the probed medium are, respectively, the electronic density (d_e) or the scattering length density (SLD, ρ_N) fluctuations, which give rise to the scattering. For a two-component medium labeled by subscripts 1 and 2, the contrast term $\Delta\rho^2$, to which scattered intensity is proportional, is simply $Ie(d_{e1} - d_{e2})^2$ for X-rays and $(\rho_{N1} - \rho_{N2})^2$ for neutrons, where Ie is the scattered intensity by a single electron ($7.9 \times 10^{-26} \text{ cm}^2$).”

(104) Gawrys, K.; Kilpatrick, P. Asphaltene aggregates are polydisperse oblate cylinders. *J. Colloid Interface Sci.* **2005**, 288, 325–334.

(105) Gawrys, K. L.; Blankenship, G. A.; Kilpatrick, P. K. Solvent entrainment in and flocculation of asphaltene aggregates probed by small-angle neutron scattering. *Langmuir* **2006**, 22 (10), 4487–4497.

(106) Barré, L.; Jestin, J.; Morisset, A.; Palermo, T.; Simon, S. Relation between nanoscale structure of asphaltene aggregates and their macroscopic solution properties. *Oil Gas Sci. Technol.* **2009**, 64, 617–628.

The likely structure for asphaltene nanoaggregates is a single disordered PAH stack in the interior with alkane substituents dominating the periphery of the nanoaggregate and with an aggregation number of ~ 7 (cf. Figure 4 and the right-hand side of Figure 24). The X-ray and neutron curves are superimposed at small q values but differ somewhat at large q .¹⁰⁶ The contrast of the SANS scattering signal, sensitive to hydrogen and, thus, alkane density, versus SAXS, sensitive to electron density and, thus, aromatic carbon (lacking hydrogen), provides a length scale of the nanoaggregate presuming the proposed structure. Figure 24 shows the length at 1.4 nm, which is very consistent with the proposed asphaltene nanoaggregate (cf. Figure 4 and the right-hand side of Figure 24).

The SANS and SAXS studies are typically performed at relatively high concentrations and in solvents different than toluene, the solvent that in part defines asphaltenes. In addition, the asphaltene nanoaggregates may have some solvent dependence. Consequently, multiple length scale nanoaggregates may exist and not be fully elucidated. For example, it is plausible that the large range of colloidal particles, 3–10 nm, from various scattering studies reflects the presence of different hierarchical structures.

In addition, SAXS and SANS measurements are sensitive to the radius of gyration while diffusion and transport terms are sensitive to the hydrodynamic radius. And measurement of size from gravitational gradients is sensitive to the physical radius in the Archimedes buoyancy term. Solvent swelling of the asphaltene nanoaggregate would impact the radius of

gyration and the hydrodynamic radius differently but would not impact Archimedes buoyancy because of cancellation in the product of density multiplied by volume. These three different radii impede direct comparison of nanoaggregate size determined by different methods.

4.2. Critical Nanoaggregate Concentration and Aggregation Number. To elucidate the crucial dynamics of asphaltene aggregation, it is necessary to determine aggregation as a function of the concentration, in particular, in toluene. Initiation of asphaltene aggregation has been shown by fluorescence quenching studies to occur at low concentrations, $\sim 50 \text{ mg/L}$.^{13,107} However, the onset of aggregation can be the formation of dimers and, therefore, does not address the CNAC, except to provide a lower limit of the CNAC concentration. Indeed, the CNAC does not define the onset of aggregation (which is not sharp in any event) but rather defines the concentration where further growth of the nanoaggregate shuts off. High-*Q* ultrasonic studies were the first to correctly determine the CNAC of asphaltenes in toluene.^{108,109} The speed of sound u is given by $u = (1/\rho\beta)^{1/2}$, where ρ is the mass density and β is the compressibility. Density is an integral property and, therefore, is not sensitive to aggregation. Compressibility is a derivative quantity and is sensitive to aggregation. The high-*Q* measurements ($Q \sim 10\,000$) afforded sufficient sensitivity to determine CNAC, as shown in Figure 25. After validation of the high-*Q* ultrasonics method on various aqueous surfactants with critical micelle concentrations (cmc's) ranging from 2.3 g/L to $\sim 10 \text{ mg/L}$, results on asphaltenes showed asphaltene CNACs at $\sim 100 \text{ mg/L}$.

The high-*Q* ultrasonics data show the CNAC for asphaltenes and also show that different asphaltenes have somewhat different values of CNAC. These differences have been confirmed by DC-conductivity measurements. For example, both high-*Q* ultrasonics and DC conductivity show that the CNAC for UG8 asphaltene is $\sim 150 \text{ mg/L}$, while for BG5 asphaltene, the CNAC is $\sim 60 \text{ mg/L}$. The significance of these differences is not known. Coal-derived asphaltenes with its much different chemical structure (cf. section 3.4) has a CNAC determined by high-*Q* ultrasonics to be 180 mg/L, which is close to that of UG8 asphaltene. Thus, there is no obvious relation between the asphaltene chemistry and the CNAC. Interestingly, DC-conductivity measurements show that, for the same crude oil, asphaltenes prepared by *n*-pentane precipitation have a significantly higher CNAC by 30% or so in concentration than the corresponding asphaltenes prepared by *n*-heptane precipitation.¹¹¹

(107) Goncalves, S.; Castillo, J.; Fernandez, A.; Hung, J. Absorbance and fluorescence spectroscopy on the aggregation of asphaltene–toluene solutions. *Fuel* 2004, 83, 1823.

(108) Andreatta, G.; Goncalves, C. C.; Buffin, G.; Bostrom, N.; Quintella, C. M.; Arteaga-Larios, F.; Perez, E.; Mullins, O. C. Nanoaggregates and structure–function relations in asphaltenes. *Energy Fuels* 2005, 19, 1282–1289.

(109) Andreatta, G.; Bostrom, N.; Mullins, O. C. High-*Q* ultrasonic determination of the critical nanoaggregate concentration of asphaltenes and the critical micelle concentration of standard surfactants. *Langmuir* 2005, 21, 2728.

(110) Zeng, H.; Song, Y. Q.; Johnson, D. L.; Mullins, O. C. Critical nanoaggregate concentration of asphaltenes by low frequency conductivity. *Energy Fuels* 2009, 23, 1201–1208.

(111) Goual, L.; Sedghi, M.; Zeng, H.; Mullins, O. C. Electrical conductivity of *n*-alkane asphaltenes and its relation to aggregation and clustering. *Energy Fuels* 2010, manuscript to be submitted.

(112) Sheu, E. Y.; Long, Y.; Hamza, H. Asphaltene self-association and precipitation in solvents—AC conductivity measurements. In *Asphaltene, Heavy Oils and Petroleomics*; Mullins, O. C., Sheu, E. Y., Hammami, A., Marshall, A. G., Eds.; Springer: New York, 2007; Chapter 10.

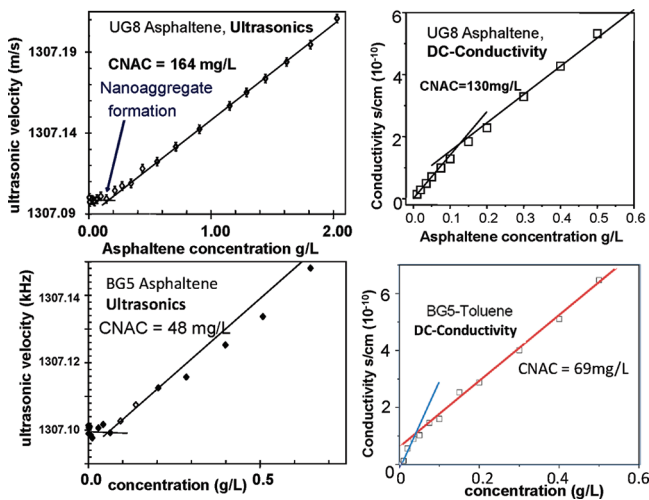


Figure 25. CNAC of asphaltenes. (Left two panels) High-*Q* ultrasonics. (Right two panels) Direct-current (DC) conductivity. The break in the ultrasonic-velocity and DC-conductivity curves show the concentration where aggregate growth stops, the CNAC. The straight line of the ultrasonic-velocity and DC-conductivity curves above the CNAC concentration indicates that the nanoaggregate size is independent of the concentration above CNAC.^{108–110} For two different asphaltenes, the CNACs differ somewhat, as shown by consistent high-*Q* ultrasonics and DC-conductivity data.

The high-*Q* ultrasonics work was first confirmed by the measurement of the AC conductivity of asphaltene solutions.¹¹² In this important work, the impedance was shown to be reactive (capacitive) and, thus, strongly dependent upon the disposition of the PAHs in the asphaltene. Very similar values of CNAC were obtained for AC conductivity in agreement with high-*Q* ultrasonics.¹¹² Also, as discussed, DC conductivity also exhibits similar CNACs.^{110,111} Possible charged groups for the DC-conductivity measurements include organic acids and pyridinium groups.¹¹³ The Bode plot was used to ensure that the impedance is in phase and, thus, resistive and not out of phase and capacitive.^{110,111} Here, electrical charge carriers in toluene experience an increase in the Stokes drag when neutral molecules aggregate onto the charged molecule. These studies show that one asphaltene molecule in 10^5 is charged in toluene and, moreover, showed that resins have a far smaller charged fraction.¹¹⁰ The electric force qE is balanced by the drag; $qE = 6\pi\eta rv$, where E is the electric field, q is the charge, η is the viscosity, r is the ion radius, and v is the velocity. Thus, the cube of the ratio of slopes gives an estimate of the aggregation number assuming that, at low concentrations, the ions are dispersed as monomers and not dimers, etc. The DC-conductivity experiments give an aggregation number of ~ 6 .^{110,111}

Many different techniques have given similar asphaltene CNACs. NMR hydrogen index measurements show the same break in the curve at roughly the same concentration for the same UG8 asphaltene as shown in Figure 26.²⁰ The reduction in signal is thought to be due to restricted asphaltene alkane diffusion upon nanoaggregate formation. This signal is rather robust; nevertheless, there is some uncertainty where the exact CNAC is (cf. Figure 26). The NMR studies also included a measurement of the concentration dependence of the asphaltene translational diffusion

(113) Kelemen, S. R.; Afeworki, M.; Gorbaty, M. L.; Kwiatek, P. J.; Solum, M. S.; Hu, J. Z.; Pugmire, R. J. XPS and ^{15}N NMR Study of Nitrogen Forms in Carbonaceous Solids. *Energy Fuels* 2002, 16, 1507–1515.

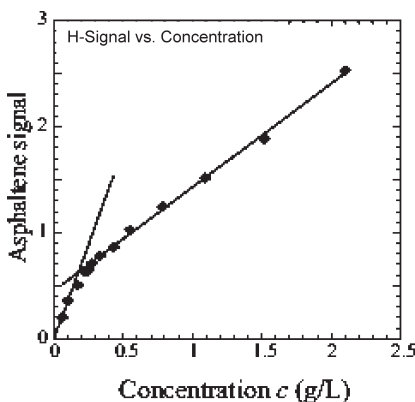


Figure 26. Concentration dependence of the ^1H NMR signal for asphaltenes. The asphaltene CNAC is seen as a break in the curve at $\sim 200 \text{ mg/L}^{20}$.

constant, while there was uncertainty why the diffusion constant showed a sudden decrease as the phase equilibrium model¹⁰⁹ showed a change in slope. Nevertheless, the decrease in the diffusion constant is roughly a factor of 2, giving an aggregation number of ~ 8 . At high concentrations, the diffusion constant showed another decline, as will be addressed.²⁰

Centrifugation studies through the same concentration range show a dramatically increasing fraction of sedimentation at the CNAC concentration, proving a significant change in aggregation at this concentration (cf. Figure 27).¹¹⁴ The centrifugation studies are very robust; there is just no doubt that the fraction of sedimented asphaltene changes dramatically at the CNAC. For the particular asphaltene shown in Figure 27, the CNAC was known from high- Q ultrasonics¹⁰⁹ and DC conductivity¹¹⁰ ($\text{CNAC} \sim 50 \text{ mg/L}$); corresponding simple models reproduced the experimental data reasonably well.¹¹⁴

Other studies that find asphaltene nanoaggregates include live crude oil centrifugation¹¹⁵ and two oil field studies examining vertically extensive crude oil columns (cf. below section 6.2).^{116,117} These studies report asphaltene gradients in crude oils under the earth's gravitational field. Larger asphaltene nanoaggregates would yield larger gradients. These studies obtain aggregation numbers less than 10.^{116,117}

Asphaltene Aggregation Number and Molecular Architecture. The small aggregation numbers for asphaltene nanoaggregates are a consequence of the molecular architecture of asphaltenes. The central PAH of the asphaltene is polarizable and, thus, the site of intermolecular attraction. In addition, virtually all of the nitrogen of asphaltene is in the aromatic core.⁷⁸ The pyridinic nitrogen is basic, and the pyrrolic nitrogen is acidic; thus, nitrogen yields some charge separation in the asphaltene PAH, increasing attractive

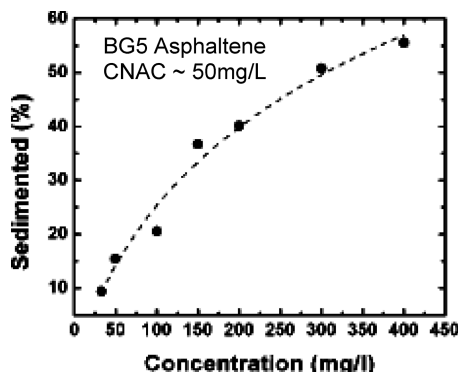


Figure 27. Percent sedimentation of asphaltenes changes dramatically at the CNAC. While the exact concentration of CNAC is not so evident here, these experiments provide robust proof that the asphaltene aggregation changes significantly in this concentration range. A two-component model, monomer and nanoaggregate, simulates the data.¹¹⁴ The CNAC for BG5 asphaltene is known from high- Q ultrasonics¹⁰⁹ and DC conductivity.¹¹⁰

intermolecular interactions. Often nitrogen is present at the $\sim 1\%$ level; thus, roughly every other asphaltene molecule has an aromatic nitrogen atom. Single-nitrogen-atom-containing asphaltene molecules greatly outnumber those with multiple nitrogen atoms.³⁹ In addition, sulfur is generally the most abundant heteroatom in asphaltenes, and a significant fraction of the sulfur is in the PAHs as thiophene.^{76,77} There is some charge separation associated with this group; dibenzothiophene has a dipole moment of $\sim 0.8 \text{ D}$ [the generally small quantity of the very polar sulfoxide group ($\sim 4 \text{ D}$) is likely aliphatic¹¹⁸]. Thus, the central PAH core is the site of polarizability and some limited charge separation.

The peripheral alkane chains and peripheral fused naphthenic rings yield steric repulsion. For example, peripheral alkanes greatly disrupt orderly stacking of aromatics, thereby dramatically lower melting points of alkylaromatics in comparison to the unsubstituted aromatics.¹¹ Because asphaltenes are a solubility class, there must be a balance of attractive forces of the PAHs and repulsive forces of the peripheral alkanes. With attractive forces in the molecular interior and repulsive forces in the molecular exterior, small aggregation numbers follow. After several asphaltene molecules aggregate, a close approach to attractive molecular real estate is obstructed and additional molecules form new nanoaggregates as opposed to adhering to existing, fully formed nanoaggregates. Molecular modeling based on these simple molecular forces gives small aggregation numbers.¹¹⁹

The term "critical" in the CNAC normally implies a sudden phase transition, and the suddenness of the aggregation process depends upon the aggregation number.¹²⁰ Smaller aggregation numbers indicate less sudden changes with the concentration.¹²⁰ As discussed above, the NMR studies, the DC-conductivity studies, the centrifugation studies, and the oilfield gravitational studies all show small

(114) Mostowfi, F.; Indo, K.; Mullins, O. C.; McFarlane, R. Asphaltene nanoaggregates and the critical nanoaggregate concentration from centrifugation. *Energy Fuels* **2009**, *23*, 1194–1200.

(115) Indo, K.; Rutulowski, J.; Dindoruk, B.; Mullins, O. C. Asphaltene nanoaggregates measured in a live crude oil by centrifugation. *Energy Fuels* **2009**, *23*, 4460–4469.

(116) Mullins, O. C.; Betancourt, S. S.; Cribbs, M. E.; Creek, J. L.; Andrews, B. A.; Dubost, F.; Venkataraman, L. The colloidal structure of crude oil and the structure of reservoirs. *Energy Fuels* **2007**, *21*, 2785–2794.

(117) Betancourt, S. S.; Ventura, G. T.; Pomerantz, A. E.; Viloria, O.; Dubost, F. X.; Zuo, J.; Monson, G.; Bustamante, D.; Purcell, J. M.; Nelson, R. K.; Rodgers, R. P.; Reddy, C. M.; Marshall, A. G.; Mullins, O. C. Nanoaggregates of asphaltenes in a reservoir crude oil. *Energy Fuels* **2009**, *23*, 1178–1188.

(118) Waldo, G. S.; Mullins, O. C.; Penner-Hahn, J. E.; Cramer, S. P. Determination of the chemical environment of sulfur in petroleum asphaltenes by X-ray absorption spectroscopy. *Fuel* **1992**, *71*, 53.

(119) Rogel, E. Molecular thermodynamic approach to the formation of mixed asphaltene–resin aggregates. *Energy Fuels* **2008**, *22*, 3922–3929.

(120) Friberg, S. E. Micellization. In *Asphaltenes, Heavy Oils and Petroleomics*; Mullins, O. C., Sheu, E. Y., Hammami, A., Marshall, A. G., Eds.; Springer: New York, 2007; Chapter 7.

aggregation numbers (< 10). For asphaltenes in toluene, the transition from a true molecular solution to nanoaggregates likely occurs over a range of concentrations and, thus, is not very sudden. Nevertheless, the term CNAC is used to indicate when nanoaggregate growth ceases.

5. Secondary Aggregation: Clusters of Asphaltene Nanoaggregates

5.1. Asphaltene Clustering Concentration. Asphaltene nanoaggregates undergo clustering at a concentration of several grams per liter. There are various lines of investigation that give rise to this conclusion. These clusters are quite small (less than 10 nm) and are *not* to be confused with flocs, which are quite large (~micrometer or more). Part of the potential confusion stems from flocculation studies that established the existence of clusters. Early experiments to clearly exhibit this phenomenon measured the flocculation kinetics of asphaltene solutions when subjected to dilution with *n*-heptane.^{121,122} Figure 28 shows the universal curve obtained for flocculation kinetics under a variety of conditions.^{121,122}

At low concentrations of asphaltene in toluene but above CNAC, asphaltenes are dispersed in toluene primarily as nanoaggregates. Upon addition of *n*-heptane, the floc formation occurs via aggregation of nanoaggregates in a process that is shown to be diffusion-limited aggregation (DLA).^{121,122} At higher asphaltene concentrations in toluene, floc growth is shown to be governed by reaction-limited aggregation (RLA).^{121,122} The interpretation of this substantial change in flocculation kinetics is that, above a certain concentration, the nanoaggregate clustering concentration, the asphaltenes are dispersed primarily as clusters of nanoaggregates. These clusters are likely fractal in their scaling.^{102,123} The cluster binding energy is much smaller than the nanoaggregate binding in accordance with the much higher clustering concentration than CNAC. Upon asphaltene destabilization by *n*-heptane addition, the clusters undergo aggregation. However, when two clusters collide, the fractal clusters might not stick, especially if the surface area of contact is low in part because of their fractal (dendritic) nature. Surface morphological change may be required to obtain sufficient adherence for floc growth. Requisite surface morphological change can appear as RLA in growth kinetics.¹²⁴ The observed transition from DLA to RLA in asphaltene flocculation kinetics is most likely due to cluster formation of nanoaggregates with a crossover concentration at ~ 5 g/L.¹²² Similar conclusions were reached in different studies of flocculation characteristics of asphaltene solutions.¹²⁵ A clear break in the

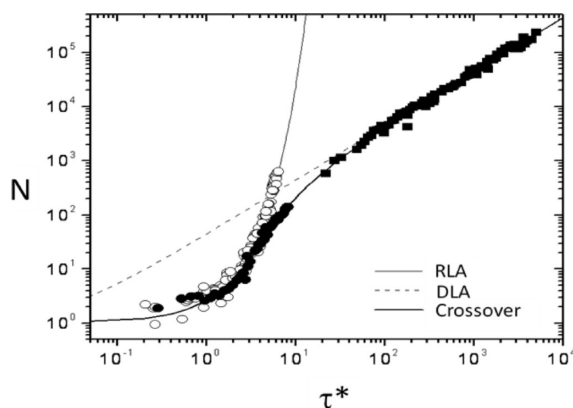


Figure 28. Aggregation number N as a function of the scaled time τ^* . Flocculation data for *n*-heptane addition to different asphaltene/toluene solutions. Open circles represent data for 10 g/L asphaltene/toluene solution exhibiting reaction-limited aggregation (RLA). Solid squares represent data for a 1 g/L asphaltene/toluene solution exhibiting diffusion-limited aggregation (DLA). Solid circles represent data for 5 g/L asphaltene/toluene solution exhibiting crossover aggregation kinetics.¹²²

flocculation behavior was obtained at 3 g/L in toluene in reasonable accordance with the kinetic studies.¹²²

Further support for a change in asphaltene colloidal dispersion has been obtained from AC-conductivity measurements.¹¹² A break in the AC-conductivity curve occurs at concentrations of several grams per liter and is consistent with a change in asphaltene colloidal dispersion at the observed clustering concentration. DC-conductivity measurements also obtain a similar break in the curve, as shown in Figure 29.^{110,111}

Figure 29 establishes that ionic conduction changes at the clustering concentration. Analysis of the ratio of the slopes of the DC-conductivity curve indicates aggregation numbers that are less than 10 nanoaggregates.^{110,111}

Surface Tension. In aqueous systems, surface tension is used regularly to measure the cmc. The idea is that the surfactant will load onto the surface of water, reducing the surface tension. At the cmc, the surfactant in the bulk forms micelles, thus without additional surfactant loading onto the water surface. When surface tension is plotted versus the natural log of the surfactant concentration, the break in the curve is the cmc. These ideas from aqueous surfactant systems were extended to look at asphaltene aggregation in pyridine with a CNAC of ~ 0.5 g/L of asphaltene in pyridine.¹²⁶ There were subsequent reports of measuring the asphaltene CNAC in toluene (or using language then in vogue, the asphaltene cmc). These reports typically obtained results on the order of several grams per liter for primary asphaltene aggregation. Of course, these high concentrations reported for asphaltene CNAC are a factor of ~ 20 higher than those from high- Q ultrasonics, NMR, AC conductivity, DC conductivity, and centrifugation, as discussed above in section 4. It was subsequently pointed out that the surface-tension measurements of asphaltene in toluene were necessarily misinterpreted.¹²⁷ The surface tension of toluene is quite low, ~ 28 dyn/cm; if a high interaction energy molecule,

(121) Anisimov, M. A.; Yudin, I. K.; Nikitin, V.; Nikolaenko, G.; Chernoutsan, A.; Toulhoat, H.; Frot, D.; Briolant, Y. Asphaltene aggregation in hydrocarbon solutions studied by photon correlation spectroscopy. *J. Phys. Chem.* **1995**, 99 (23), 9576–9580.

(122) Yudin, I. K.; Anisimov, M. A. Dynamic light scattering monitoring of asphaltene aggregation in crude oils and hydrocarbon solutions. In *Asphaltenes, Heavy Oils and Petroleomics*; Mullins, O. C., Sheu, E. Y., Hammami, A., Marshall, A. G., Eds.; Springer: New York, 2007; Chapter 17.

(123) Sheu, E. Y. Petroleum asphaltene—Properties, characterization, and issues. *Energy Fuels* **2002**, 16, 74–82.

(124) Mullins, W. W. Private communication. Carnegie-Mellon University, Pittsburgh, PA.

(125) Oh, K.; Deo, M. D. Near infrared spectroscopy to study asphaltene aggregation in solvents. In *Asphaltenes, Heavy Oils and Petroleomics*; Mullins, O. C., Sheu, E. Y., Hammami, A., Marshall, A. G., Eds.; Springer: New York, 2007; Chapter 18.

(126) Sheu, E. Y.; De Tar, M. M.; Storm, D. A. Surface activity and dynamics of asphaltenes. In *Asphaltene Particles in Fossil Fuel Exploration, Recovery, Refining, and Processing Processes*; Sharma, M. K., Yen, T. F., Eds.; Springer: New York, 1994; p 115.

(127) Friberg, S. E.; Mullins, O. C.; Sheu, E. Y. Surface activity of an amphiphilic association structure. *J. Dispersion Sci. Technol.* **2005**, 26, 513–515.

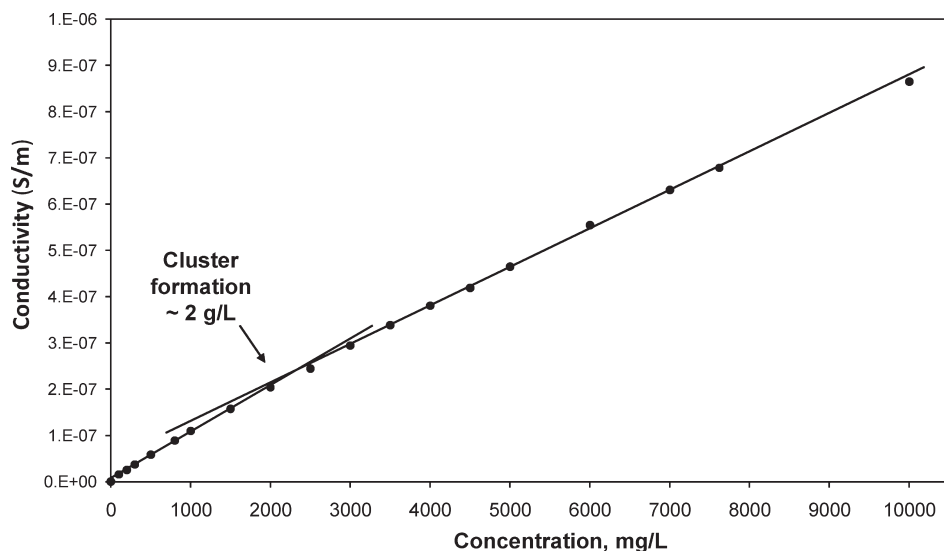


Figure 29. DC conductivity for an asphaltene exhibits a significant reduction of slope at ~ 2 g/L (in addition to the change of slope at the CNAC at ~ 150 mg/L).¹¹¹ The change in slope is quite evident but not large, indicating that the cluster aggregation numbers are not large.¹¹¹ The constant slope at concentrations above the clustering concentration indicates that the cluster size does not change with the concentration in this range.¹¹¹

such as asphaltene, goes to the surface of toluene, the surface tension will go up and not down, as was measured.¹²⁷ It was also shown with a model system that, if an invert micelle goes to the surface of toluene, the surface tension will be reduced because of the outwardly projecting alkanes.¹²⁸ The asphaltene nanoaggregate also has outwardly projecting alkanes. It is most likely that the surface-tension measurements of asphaltene in toluene were misinterpreted; the measurements were sensitive to the clustering concentration and not the CNAC. We also view that the calorimetric measurements that initially indicated an asphaltene cmc of several grams per liter were likely responding to the clustering concentration.¹²⁹ More recent calorimetric measurements do not see a clear break at the CNAC.¹³⁰ The CNAC is partially entropy-driven (positive entropy of aggregation),²⁰ which would not be observed by calorimetry. In conclusion, the surface tension and calorimetry studies evidently show effects at the clustering concentrations; we view this as corroborative. The role of water in asphaltene aggregation has been observed to be significant.¹³¹ Water is present in oilfields, and thus, in crude oils; therefore, its role in aggregation needs to be considered.

5.2. Cluster size. It is important to determine the size of the nanoaggregate clusters. The clusters must be larger than the nanoaggregates (~ 2 nm) and smaller than flocs. When conditions are adjusted to favor slightly the formation of flocs (by dropping the pressure slightly below the onset pressure), then smaller flocs form. These small flocs have been measured to be ≥ 300 nm by both the wavelength

dependence in light scattering and the sedimentation rate, thus establishing an upper limit for the size of asphaltene clusters.¹³² Ultrafiltration studies of very high-concentration asphaltic systems at very high temperatures have obtained asphaltenes being retained on filters with 100 nm nominal pore size.¹³³ More asphaltenes are retained on filters with smaller pore size, suggesting a range of cluster sizes.¹³³ These experiments employed a large filtration pressure drop and, therefore, had to have robust and, thus, somewhat thick porous ceramic frit filters.¹³³ There can be particle jamming in porous media. The cluster size might be rather dependent upon the temperature (presumably smaller at high T) and concentration (presumably larger at higher concentrations).

Recently, nanofiltration experiments have been performed with Gore-Tex Teflon filters of 30 nm nominal pore size.¹³⁴ The pore size was confirmed using filtration of polystyrene spheres of known size.¹³⁴ Both dead crude oils and asphaltene–toluene solutions have been filtered.¹³⁴ The crude oils were filtered at elevated temperature ($T = 80$ °C) to preclude wax formation, while the toluene solutions were filtered at room temperature.¹³⁴ The pressure differential for filtration was less than 1 atm. For the crude oils and asphaltene solutions, there was no detectable change in the coloration of the liquid/solution before and after filtration and there was no observed retentate on the filter. The highest asphaltene content for crude oils was 8%. In addition, the viscosity of the crude oils was measured before and after filtration and was found to be the same.¹³⁴ No disruption of the colloidal structure of asphaltene could be registered in the viscosity.¹³⁴ It has been established that some asphaltene kinetics are very slow (months),¹³⁵ making this viscosity measurement relevant (nevertheless, the viscosities of very

(128) Friberg, S. E.; Al Bawab, A.; Abdoh, A. A. Surface active inverse micelles. *Colloid Polym. Sci.* **2007**, *285*, 1625–1630.

(129) Andersen, S. I.; Christensen, S. D. The critical micelle concentration of asphaltenes as measured by calorimetry. *Energy Fuels* **2000**, *14*, 38–42.

(130) Merino-Garcia, D.; Andersen, S. I. Application of isothermal titration calorimetry in the investigation of asphaltene association. In *Asphaltenes, Heavy Oils and Petroleomics*; Mullins, O. C., Sheu, E. Y., Hammami, A., Marshall, A. G., Eds.; Springer: New York, 2007; Chapter 13.

(131) Khvostichenko, D. S.; Andersen, S. I. Interactions between asphaltenes and water in solutions in toluene. *Energy Fuels* **2008**, *22*, 3096–3103.

(132) Joshi, N. B.; Mullins, O. C.; Jamaluddin, A.; Creek, J.; McFadden, J. Asphaltene precipitation from live crude oils. *Energy Fuels* **2001**, *15*, 979.

(133) Zhao, B.; Shaw, J. S. Composition and size distribution of coherent nanostructures in Athabasca bitumen and Maya crude oil. *Energy Fuels* **2007**, *21*, 2795–2804.

(134) Ching, M.-J. T. M.; Pomerantz, A. E.; Andrews, A. B.; Dryden, P.; Mullins, O. C.; Harrison, C. On the nanofiltration of asphaltene solutions, crude oils and emulsions. *Energy Fuels* **2010**, manuscript submitted.

(135) Maqbool, T.; Balgoa, A. T.; Fogler, H. S. Revisiting asphaltene precipitation from crude oils: A case of neglected kinetic effects. *Energy Fuels* **2009**, *23*, 3681–3686.

concentrated asphaltic systems are shown to be described by a slurry of Newtonian fluids, and a solid of non-interacting spheres providing the solid content of the particular maltenes is properly taken into account¹³⁶.

Figure 30 shows that there is no detectable loss of asphaltene upon filtration of the asphaltene–toluene solutions; the pre- and postfiltration solutions have spectra that overlay. These data might appear to be contradictory to previous ultrafiltration studies.¹³³ However, the conditions of the two sets of ultrafiltration studies are quite different. In any event, the upper size limit of less than 30 nm established here for clusters is consistent with the small change in slope in the DC-conductivity measurements for the same asphaltene (UG8) in toluene (cf. Figure 29).^{110,111}

6. Applications of the Modified Yen Model

6.1. Asphaltene Interfacial Science. First and foremost, the modified Yen model enables a great deal of wide-ranging data at multiple length scales to be understood within a relatively simple context. Indeed, it is our hope that all of the above sections have made that clear. We also note that workers in the field are adopting the language “modified Yen model.” For example, to understand the governing principles of asphaltene PAHs, explicit use is made of the modified Yen model, explaining both the electronically excited singlet¹³⁷ and triplet¹³⁸ states of PAHs. This is at the molecular length scale. At the nanoaggregate length scale, the contrasting SANS and SAXS spectra (as presented in Figure 24) also employ similar language.¹⁰⁶ This is, of course, at the nanoaggregate length scale.

One of the most challenging issues to address for asphaltene science and thus for the modified Yen model is interfacial science. Interfacial phenomena can be dominated by components present in a very small mass fraction. In addition, there is very little material at the interface precluding use of many characterization methods. Recent work uses the modified Yen model to understand asphaltene interfacial science.

Sum frequency generation (SFG) is a method designed to interrogate the interface.¹³⁹ In particular, these very difficult experiments, especially when applied to asphaltenes, can yield molecular orientation at the interface. A tunable IR laser overlaps a visible laser at the interface. Sum frequency generation can occur as a function of several constraints. The cross-section contains a product of the IR-allowed and Raman-allowed transitions. In addition, the symmetry must be low enough in the interrogated volume, or cancellation precludes obtaining any SFG signal. For surface molecular layers, often only the surface is SFG-active, a very desirable trait for surface investigation. Langmuir–Blodgett films of

(136) Hasan, M. D. A.; Fulem, M.; Bazyleva, A.; Shaw, J.M. Rheological properties of nanofiltered Athabasca bitumen and Maya crude oil. *Energy Fuels* 2009, 23, 5012–5021.

(137) Ruiz-Morales, Y. Aromaticity in pericondensed polycyclic aromatic hydrocarbons determined by density functional theory nucleus-independent chemical shifts and the Y-rule—Implications in oil asphaltene stability. *J. Can. Phys.* 2009, 87, 1280–1295.

(138) Barrasso, E.; Klee, A.; Masterson, T.; Ruiz-Morales, Y.; Mullins, O. C.; Lepkowicz, R. Electronic triplet states of asphaltenes. Manuscript in preparation.

(139) Andrews, A. B.; McClelland, A.; Korkeila, O.; Demidov, A.; Krummel, A.; Mullins, O. C.; Chen, Z. Sum frequency generation studies of Langmuir films of complex surfactants and asphaltenes. *J. Am. Chem. Soc.* 2010, manuscript submitted.

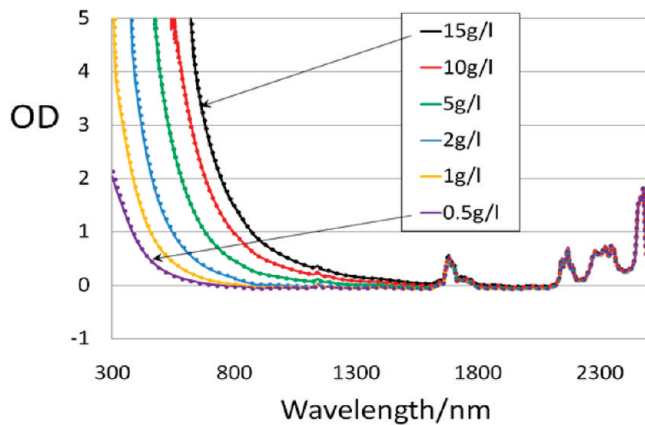


Figure 30. Optical spectra for solutions before and after filtration overlay for various asphaltene–toluene solutions. The smooth increasing absorption in the spectral range (here) between 300 and 1300 nm corresponds to electronic transitions of asphaltenes; the optical density (OD) is linearly dependent upon the asphaltene concentration (the peaks at longer wavelength correspond to overtone vibrational transitions of the solvent toluene). Room-temperature filtration had no effect on the color (electronic absorption) of the solutions. The nominal pore size of the Gore-Tex Teflon filter was 30 nm. The implication is that clusters of asphaltene nanoaggregates, which form at several grams per liter concentration, are much smaller than 30 nm.¹³⁴

heteroatomic alkyl aromatics have been measured using SFG.¹³⁹ When the SFG signal is measured as a function of S and P polarization of the incident laser beams and the SFG sum frequency beam, molecular orientation at the interface can be investigated.

Figure 31 shows that complex surfactants exhibit molecular alignment in Langmuir–Blodgett films. The surfactant used for Figure 31 has a carboxylic acid that likely dominates the molecular orientation at the interface. The SFG data suggest that the PAH of C5Pe surfactant is largely perpendicular to the interface. Little net orientation of terminal methyls is indicated¹³⁹ (the methylene SFG signal can cancel for trans configuration with sufficient chain length.¹³⁹).

Figure 32 shows preliminary yet very interesting SFG data for a Langmuir–Blodgett film of asphaltenes from an air–water interface prepared from a ~0.2 mg/L solution. This concentration is much lower than the CNAC; thus, a molecular dispersion of asphaltene in the Langmuir film is expected. Possibly the surface compression prior to isolation of the Langmuir–Blodgett film causes some aggregation. Most importantly, the asphaltenes appear to be anisotropic and, thus, molecularly aligned at the interface. The data suggest that the asphaltene PAHs are parallel to the interface, while the asphaltene alkanes appear to be perpendicular to the interface. This is consistent with the highest energy region of the asphaltene molecules being the PAH, a concept that arises repeatedly with the modified Yen model. These SFG data are inconsistent with the archipelago model with multiple small PAHs; the ordering of the PAHs would be much less.

Langmuir films of asphaltenes on water have been prepared in the concentration range where nanoaggregates are expected.^{140,141} For asphaltene Langmuir films on water

(140) Orbulescu, J.; Mullins, O. C.; Leblanc, R. M. Surface chemistry and spectroscopy of UG8 asphaltene, Langmuir film, Part 1. *Langmuir* 2010, manuscript to be submitted.

(141) Orbulescu, J.; Mullins, O. C.; Leblanc, R. M. Surface chemistry and spectroscopy of UG8 asphaltene Langmuir film, Part 2 *Langmuir* 2010, manuscript to be submitted.

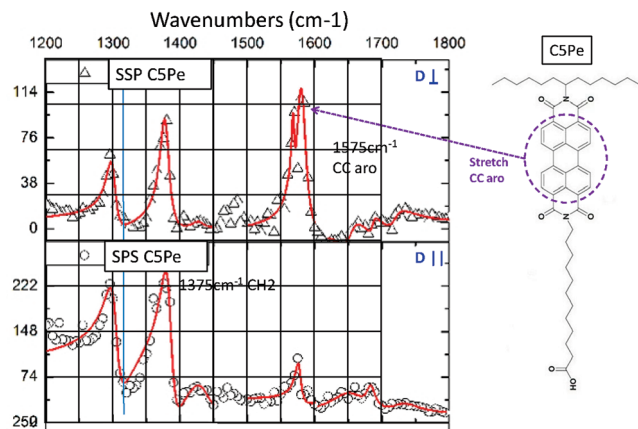


Figure 31. SFG spectra of a Langmuir–Blodgett film prepared from an air–water interface of the compound labeled C5Pe for the (top) SSP and (bottom) SPS polarizations of the tunable IR laser, visible laser, and sum frequency beam. A strong orientation of the PAH ring system largely perpendicular to the surface is suggested.¹³⁹

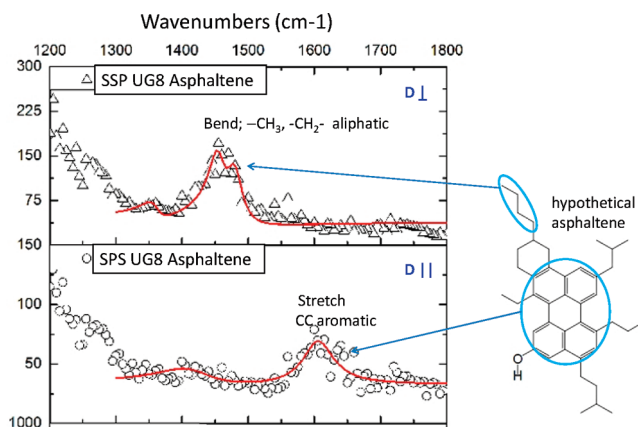


Figure 32. Preliminary SFG data for a Langmuir–Blodgett film of UG8 asphaltene prepared from an air–water interface using a ~0.2 mg/L toluene solution.¹³⁹ The SFG data suggest that the asphaltene PAH is parallel to the interface, while the asphaltene alkanes are perpendicular.

prepared from toluene solutions, the surface area per molecule is measured to be ~19 Å²,¹⁴⁰ for molecules in the range of 14 Å dimension (with considerable anisotropy), this is consistent with aggregation numbers of ~10. In addition, infrared spectroscopy of the Langmuir film showed that the IR bands did not exhibit the normal shift upon surface area compression, indicating that the asphaltenes are already aggregated prior to compression,¹⁴⁰ in agreement with reported CNACs elsewhere (cf. section 4). In addition, the UV–vis spectrum was obtained for the asphaltene Langmuir films on water, as shown in Figure 33. At short times (15 min) after film preparation, there is a persistent absorption band of toluene in the spectrum (Figure 33A), indicating that toluene did not yet evaporate. After waiting 1 h, there are very small toluene peaks slightly shifted from that obtained at 15 min (cf. Figure 33B) and are thought to reflect toluene entrained in the asphaltene nanoaggregates.¹⁴¹ A similar conclusion has been obtained from SANS studies of asphaltene;¹⁰⁵ the optical data show support for this conclusion. Surface studies here establish that single-ring aromatics can

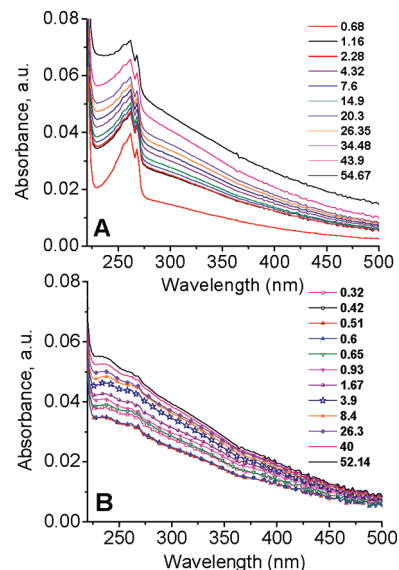


Figure 33. UV–vis absorption of the asphaltene Langmuir film on water for different surface compressions (dyn/cm) with (A) 15 min wait time before compression and (B) 60 min wait time.¹⁴⁰ The persistent toluene peak at 260 nm in spectra A shows that toluene has not yet evaporated completely. The tiny toluene peaks at 1 h are thought to reflect toluene entrained in the asphaltene nanoaggregates.¹⁴⁰ These peaks do not appear in asphaltene Langmuir films prepared from chloroform.¹⁴¹

readily be observed (Figure 33A) and that asphaltenes do not exhibit this single-ring aromatic peak in significant strength (Figure 33B).¹⁴⁰

Langmuir films of asphaltene on water have also been prepared from chloroform.¹⁴¹ There is virtually no other literature on the state of asphaltene aggregation in chloroform. A compression of the Langmuir film on chloroform consistently gives a much larger area per molecule of ~40 Å², indicating that the asphaltene nanoaggregates in chloroform are smaller than those in toluene.¹⁴¹ In addition, the UV–vis absorption spectra for this asphaltene Langmuir film showed smaller absorbances than the corresponding film prepared from toluene, in support of the smaller aggregation size for the asphaltene nanoaggregates in chloroform. The asphaltene spectra of Langmuir films obtained from chloroform solutions did not exhibit any peaks associated with single-ring aromatics, indicating that asphaltenes have a very small mass fraction of single-ring aromatic PAHs.¹⁴¹ This observation also supports the interpretation that the small toluene peak in Figure 33B is from entrained toluene in the nanoaggregate. In contrast to large fused ring systems where spectral profiles merge for different PAHs, there is a big difference between single- and two-ring aromatics; consequently, peaks from single-ring aromatics can be observed if present.⁷³ The lack of significant single ring aromatics has also been obtained by molecular orbital (MO) analysis of asphaltene absorption and fluorescence emission spectra as well as TRFD studies of asphaltenes (cf. section 3.2). These studies of asphaltene Langmuir films provide strong support for previous determinations of asphaltene molecular architecture and nanoaggregate size and are very compatible with the modified Yen model. The modified Yen model provides a successful framework to interpret substantial new data obtained for asphaltene interfacial science with multiple solvents.

Other studies carried out on Langmuir films of asphaltenes at higher concentrations are also very consistent with the modified Yen model and also yield fascinating results.¹⁴² Langmuir films of asphaltene on water were prepared from asphaltene toluene solutions above and below the clustering concentration.¹⁴² The films were analyzed by Brewster angle microscopy (BAM). The BAM images are shown in Figure 34 for clusters (on the left) and nanoaggregates (on the right) for various surface pressures and asphaltene coverages. The huge difference is directly attributed to the difference in bulk dispersion of asphaltenes, cluster versus nanoaggregates, and is described within the modified Yen model.¹⁴²

The extension of the modified Yen model to describe interfacial behavior of asphaltenes in these studies is a very important advance and relates to wettability and, thus, enhanced oil recovery, in addition to emulsion stability. The surface morphology of asphaltene films can undergo complex time evolution,¹⁴³ and interfacial properties of crude oils have many dependencies and not just asphaltenes.¹⁴⁴ Nevertheless, the successful application of the modified Yen model for understanding major aspects of asphaltene Langmuir films is very important and represents considerable success for the modified Yen model.¹⁴²

6.2. Oilfield Reservoir Characterization. In the past, there have been two confounding assumptions made about oilfield reservoirs that have often been proven incorrect; the assumptions had been that the contained crude oils were largely homogeneous and that the subsurface compartments that contained the fluids are very large¹⁴⁵ (a compartment is an oil-bearing rock formation that must be penetrated by a well to drain). Indeed, these assumptions were routinely made in particular oilfields, but often production shortfalls and other production problems arose, proving these twin simplicities false. With the major global play of deepwater oil production, the failure of assumptions can no longer be tolerated. For deepwater, well costs and subsea facilities contribute to massive expense. Frequently, on the order 90% of the capital expense of an oil production project is spent *prior* to first oil. In this setting, it is essential to assess prior to production the types of fluids that are to be produced and to assess the extent of flow connectivity in the reservoir.

Fluid compositional variation is best illustrated by a photograph of dead crude oil samples from a single column of oil (cf. Figure 35).^{145,146} The primary visual cue that is being observed in Figure 35 is the asphaltene content. These crude oil samples are dead, that is, exposed to one atmosphere pressure; therefore, their dissolved gases have been released. In the subsurface formation, the samples on the right have much more dissolved gas than those on the left; therefore, for the live crude oils, with their dissolved gas, the color gradient would appear even larger.

To perform measurements of oil properties in reservoirs, it is most cost-effective to perform the measurements *in situ* in oil wells. An “open hole” sampling tool is used to acquire

(142) Lobato, M. D.; Pedrosa, J. M.; Möbius, D.; Lago, S. Optical characterization of asphaltenes at the air–water interface. *Langmuir* 2009, 25, 1377–1384.

(143) Sztukowski, D. M.; Yarranton, H. W. Rheology of asphaltene–toluene/water interfaces. *Langmuir* 2005, 21 (25), 11651–11658.

(144) Czarnecki, J. Stabilization of water in crude oil emulsions. Part 2. *Energy Fuels* 2009, 23, 1253–1257.

(145) Mullins, O. C. *The Physics of Reservoir Fluids; Discovery through Downhole Fluid Analysis*; Schlumberger Press: Houston, TX, 2008.

(146) Elshahawi, H. Shell Exploration and Production Company, Inc., Houston, Texas.

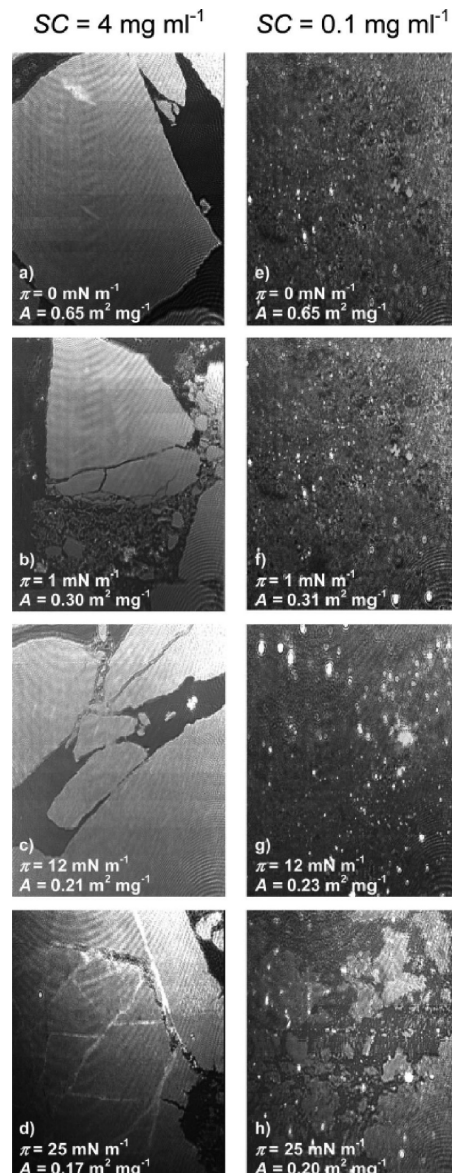


Figure 34. BAM images of asphaltene Langmuir films obtained from two different spreading concentrations (SCs), 4 g/L (left, images a–d) and 0.1 g/L (right, images e–h), at different surface pressures, π , on water.¹⁴² The corresponding values of specific area (m^2/mg) are also indicated in the images. Image size = 430 μm width.

ire fluid samples prior to placing steel casing in the well. Figure 36 shows a photograph and schematic of such a tool.

Figure 36 shows that the sample acquisition tool has multiple optical spectrometers on board to perform fluid analysis as the formation fluid is pumped through the optical cells.¹⁴⁵ The optical measurements include NIR spectroscopy for determination of various hydrocarbon constituents, optical coloration for determination of the heavy-end content, and fluorescence measurements.¹⁴⁵ These measurements are subsumed under the heading “downhole fluid analysis” (DFA), which incorporates a growing list of chemical and physical measurements of fluid properties for a multitude of purposes.¹⁴⁵

The formation sampling and analysis tool depicted in Figure 36 is important for reservoir evaluation. Figure 37 depicts the upper and lower reservoir surfaces of the Tahiti



Figure 35. Series of dead crude oil samples obtained from a single oil column visually showing the huge variation of crude oil properties that can occur (courtesy of Hani Elshahawi, Shell Exploration and Production). Here, the huge variation in asphaltene content is the visual cue depicting the gradient.

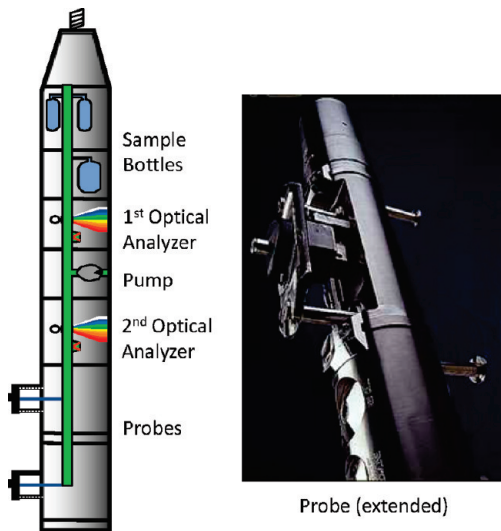


Figure 36. Schematic of an “open hole” downhole sampling and fluid analysis tool and a photograph of the probe (extended), which makes contact with the borehole wall and establishes hydraulic communication with the oil-bearing subsurface formation. This tool is used in open hole, prior to casing the well sections of interest. The formation crude oil is brought into the tool, and various optical measurements are performed to measure chemical properties and constituents (cf. ref 145 and references therein).

field, deepwater Gulf of Mexico. The field is tilted primarily because of buoyant (allochthonous) salt.¹⁴⁷ Obviously, the field is not rigid; therefore, faulting occurs during this process. It is critical for facile drainage of the field that these faults are transmissive and not sealing barriers for fluid flow. In addition, other, much thinner sealing barriers can occur in the field, generally making compartmentalization the biggest risk factor globally in deepwater oil production.¹⁴⁵

One method to assess reservoir connectivity is to determine whether the reservoir fluids show sharp discontinuous or continuous behavior vertically and laterally in the reservoir. Of course, discontinuous behavior argues for the existence of sealing barriers. Continuous fluid properties tend to suggest connectivity.¹⁴⁵ In particular, if the reservoir fluids are in thermodynamic equilibrium vertically and laterally, then there is a stronger case for connectivity. The fluids necessarily enter the reservoir out of ultimate equilibrium; therefore, establishing fluid equilibrium in the reservoir requires massive fluid flow and suggests reservoir connectivity.¹⁴⁵ Still, the time frame to establish equilibrium

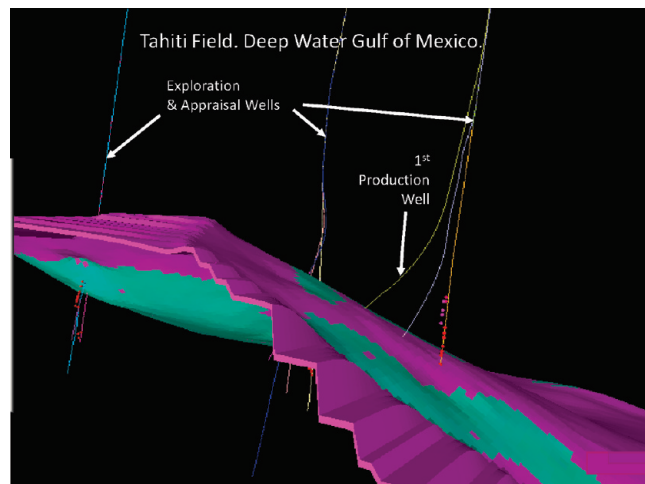


Figure 37. Upper and lower surfaces of the Tahiti reservoir, deep-water Gulf of Mexico. The field is at a depth > 20 000 ft and water depth of ~4000 ft. Various oil wells are shown. The tool depicted in Figure 36 is used to assess the nature of fluids in the reservoir.^{116,145}

is much longer than production times; thus, caution is urged at every step of the evaluation.

Light crude oils with a large dissolved gas content are expected to exhibit large compositional gradients.^{148,149} The large dissolved gas fraction causes the corresponding fluid to have large compressibility. Consequently, the hydrostatic head pressure from the oil column causes the fluid at the base of the column to have a higher density. The density gradient in the oil column produces the thermodynamic drive to create a compositional gradient, with high-density components accumulating toward the base and low-density components accumulating toward the top of the column in accordance with Le Chatelier’s principle.^{145,148,149} Consequently, equilibrium distributions of high gas/oil ratio (GOR) fluids in the reservoir are characterized by large gradients of GOR (the GOR is a ratio of the gas to liquid volumes of the reservoir oil when under conditions of 1 atm and 60 °F). Standard equations of state are routinely used to evaluate whether reservoir fluids are in equilibrium, thereby helping to assess reservoir connectivity.

However, for black oils of low GOR, there had been uncertainty for how to proceed. Low GOR crude oils have low compressibility; thus, they have small GOR gradients. The largest gradients for these oils are often in the asphaltenes. However, the colloidal structure of asphaltenes had

(147) Dribus, J.; Jackson, M. P. A.; Kapoor, J.; Smith, M. *The Prize Beneath the Salt, Oilfield Review*; Schlumberger Press: Houston, TX, Autumn, 2008.

(148) Hoier, L.; Whitson, C. Compositional grading, theory and practice. *SPE Reservoir Eval. Eng.* **2001**, 525–535.

(149) Ratulowski, J.; Fuek, A. N.; Westrich, J. T.; Sieler, J. J. Theoretical and experimental investigation of isothermal compositional grading. *SPE Tech. Pap.* 84777, Dallas, TX, 2003.

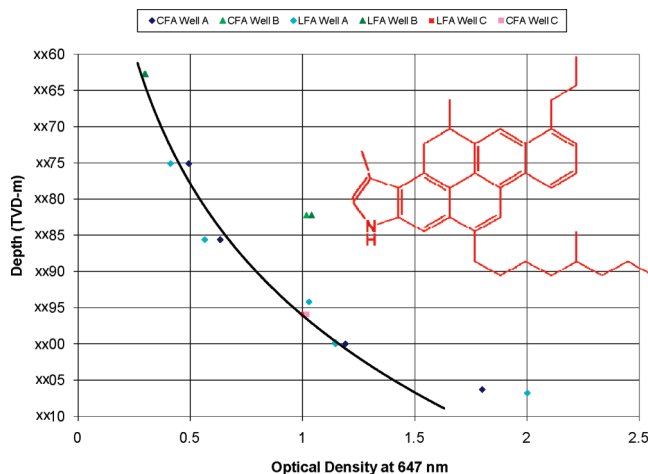


Figure 38. Coloration profile obtained in three wells in a nominally single reservoir showing a continuous coloration profile for most data points.¹⁵⁰ Modeling this profile gave a “particle” size of 1.3 nm, indicating that the coloration profile is predominantly due to a molecular dispersion of asphaltene-like resin molecules (embedded in the figure). By asphaltene-like resin molecules, we mean molecules with color (thus, asphaltene-like) but which are *n*-heptane-soluble (thus, resin). The LFA and CFA are two DFA tools that are used to measure color, here, redundantly.

been unknown; thus, the gravity term could not be understood. Consequently, methods to exploit heavy ends for connectivity analysis were not developed. Indeed, the Yen model was not of use to understand the colloidal dispersion of asphaltenes in crude oil. In addition, the Yen model was of no use for reservoir evaluation.

The modified Yen model provides a framework for understanding the molecular and/or colloidal dispersion of heavy ends in crude oil. Moreover, the new technology DFA provides a measurement of oil coloration *in situ* in oil wells, thereby obtaining the relative heavy-end concentration. The combination of the modified Yen model and DFA provides the means to evaluate connectivity and other complexities in reservoirs.

For light reservoir fluids, such as condensate, asphaltenes are virtually absent and there is not much coloration. The coloration that is present is in the visible wavelength range, where the smaller PAHs of the colored resins absorb. The large GOR gradient of these compressible fluids yields a large variation in the solubility parameter, thereby driving the color gradient. Figure 38 shows the coloration of a condensate in a nominally single reservoir intersected by three different wells A, B, and C. Most of the DFA-measured color points are on a continuous curve, implying reservoir connectivity.¹⁵⁰ The two outliers (at xx82 and xx06 m) are at the base of the producing sands in two wells and exhibit too much color. The origin of this effect is under investigation.¹⁵⁰

Figure 39 shows crude oil coloration data from the Tahiti reservoir (cf. Figure 37). The asphaltene content varies by a factor of ~2.5 over 3000 ft vertically. The M21A and M21B sands are the two primary reservoir sands but are not in pressure communication and, thus, are not in flow communication. Pressure communication is a necessary but not

(150) Gisolf, A.; Dubost, F.; Zuo, J.; Williams, S.; Kristoffersen, J.; Achourou, V.; Bisarah, A.; Mullins, O. C. Real time integration of reservoir modeling and formation testing, SPE Tech. Pap. 121275, SPE EUROPEC/EAGE Annual Conference and Exhibition, Amsterdam, The Netherlands, 2009.

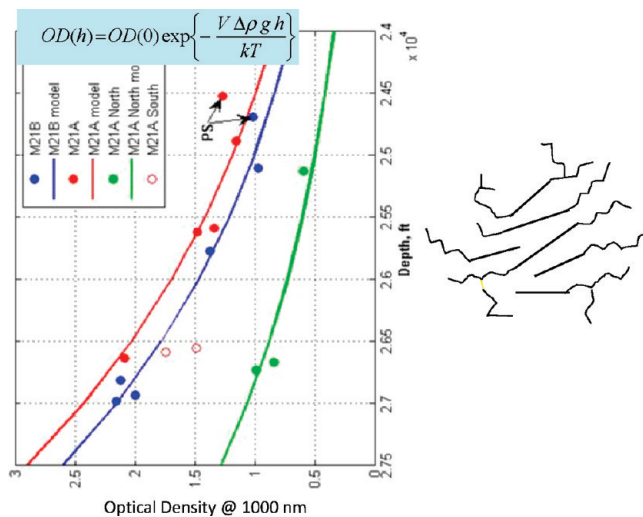


Figure 39. Coloration profile of crude oils in the Tahiti reservoir, deepwater Gulf of Mexico.¹¹⁶ The red and blue curves correspond to two different sands that are not in pressure communication and, therefore, not in flow communication. The embedded equation in the figure was used to fit the data, giving an asphaltene nanoaggregate (on the right of the figure) solid sphere diameter of 1.6 nm.¹¹⁶

sufficient condition to establish flow communication. Most of the data from the field lie on the theoretical fit curves obtained from the gravitational gradient model of asphaltene nanoaggregates.¹¹⁶ The GOR of the crude oil is low and, therefore, relatively uniform. Production from this field confirms that reservoir connectivity is found when the reservoir fluid is in equilibrium.

Figure 40 shows a much larger asphaltene gradient, a factor of 10 for the asphaltene concentration in 100 m vertically. The gradient in the asphaltene content can be fitted by an equation with 90% of 2 nm asphaltene nanoaggregates and 10% of 4 nm asphaltene clusters. The nanoaggregates are the familiar 2 nm in diameter, while the nanoaggregate clusters are ~4 nm for a solid sphere. If the cluster is fractal, its physical size would be closer to 6 nm.

We believe the clusters represent a partially destabilized asphaltene in this oil column. Asphaltenes are polydisperse, with differing levels of stability. Upon destabilization, some asphaltenes form clusters, while less stable fractions can phase-separate. Several observations have been made in this field in support of this model: (1) a nearby well has the reservoir pressure equal to the asphaltene onset pressure (with no pressure depletion during production); (2) there is bitumen in the core, indicating that some asphaltenes were phase-destabilized; (3) the oil did develop asphaltene flocs upon depressurization, indicating that some asphaltene instability; and (4) the analysis of the toluene versus *n*-heptane content in the oil is consistent with some gas washing, which could lead to asphaltene destabilization.

The analysis of crude oil and asphaltene “coloration”, that is, the strength of electronic transitions of chromophores, for reservoir evaluation, makes the assumption that the color is linear in asphaltene content. Figure 41 shows that the live crude oil coloration measured by DFA matches the laboratory measurement of the asphaltene content.

The *y*-axis intercept of the linear relationship of color versus asphaltene content is not at the origin. There is a small fraction of resins that are (visually) colored as well.

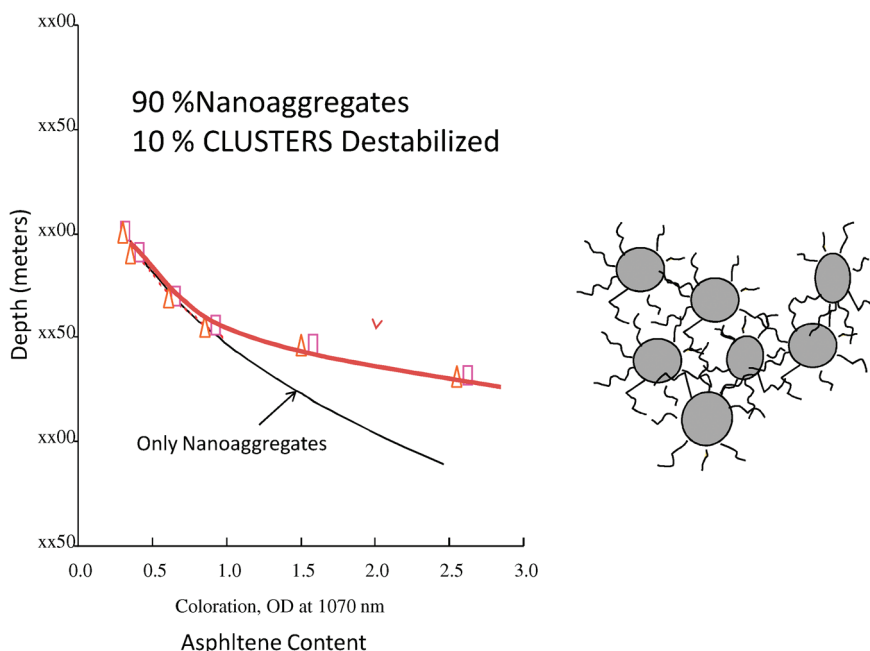


Figure 40. Very large asphaltene gradient in a subsurface reservoir thought to be due to the presence of both asphaltene nanoaggregates and nanoaggregate clusters in the reservoir crude oil. A cluster is depicted in the figure.

On average, the resin PAHs are smaller than those of asphaltenes. Thus, the resin electronic absorption spectra are blue-shifted relative to asphaltenes (cf. Figure 11). Consequently, for a given crude oil, the fraction of electronic absorption due to the asphaltenes versus the colored resins increases at longer wavelengths. It is likely that different fields will give a different slope to the corresponding plots similar to Figure 41; thus, DFA coloration measures relative asphaltene content within a field.

7. Asphaltene–Resin Interaction

The modified Yen model does not explicitly address the extent of the asphaltene–resin interaction. However, the modified Yen model does treat the formation of asphaltene nanoaggregates and nanoaggregate clusters without invoking any resin interaction. Thus, the classic view of the “surfactant resin” for asphaltene nanoaggregates is incompatible with the modified Yen model. Nevertheless, this resin issue has been of concern since the earliest days of establishing the field of asphaltene science. This is another area where significant progress has been made, albeit not fully resolved. When asphaltene science was in its infancy, it was stated that asphaltenes are colloidally suspended in crude oil.^{151,152} Many sections of this paper argue that this early colloidal statement is indeed correct and represents significant success for these earlier researchers. It was also stated without demonstration that asphaltene colloidal particles are stabilized by a coating of resin molecules; thus, the conjecture is that resins act as surfactants for asphaltenes in crude oil.^{151,152} The idea is that colloidal systems have large interfacial area and interfacial energy. If such a system is stable for geologic time, then there must be a clear origin to this stability. Aqueous colloidal stabilization in micelles is well-known. Oil-in-water emulsions

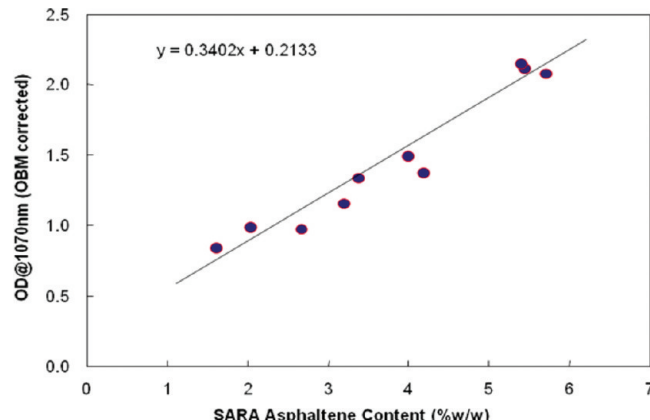


Figure 41. Coloration of a black crude oil is linear in the asphaltene content as measured by the laboratory. This linear relation is very useful for application of DFA for reservoir evaluation.¹⁴⁵

can be stabilized by charged surfactants; the like-charged colloidal particles repel precluding coalescence. This micelle picture has been promulgated for asphaltene colloidal particles with resins proposed as the surfactants, although the possible role of electric charge was left unaddressed. Corresponding cartoons have been published ubiquitously in asphaltene literature (and pointedly not copied here) lending credence to these ideas. Nevertheless, modeling phase behavior of asphaltenes does not require resin participation, and indeed, there is almost no data supporting the “peptizing resin” assertions.^{153,154} As Buckley and co-authors state

(151) Nellensteijn, F. I. In *The Science of Petroleum*; Dunstan, A. E., Ed.; Oxford University Press: London, U.K., 1938; Vol. 4.

(152) Pfeiffer, J. P.; Saal, R. N. Asphaltic bitumen as colloid system. *J. Phys. Chem.* **1940**, *44*, 139.

(153) Cimino, R.; Correra, S.; Del Bianco, A.; Lockhart, T. P. Solubility and phase behavior of asphaltenes in hydrocarbon media. In *Asphaltenes, Fundamentals and Applications*; Sheu, E. Y., Mullins, O. C., Eds.; Plenum Press: New York, 1995; Chapter 3.

(154) Buckley, J. S.; Wang, X.; Creek, J. L. Solubility of the least-soluble asphaltenes. In *Asphaltenes, Heavy Oils and Petroleomics*; Mullins, O. C., Sheu, E. Y., Hammami, A., Marshall, A. G., Eds.; Springer: New York, 2007; Chapter 16.

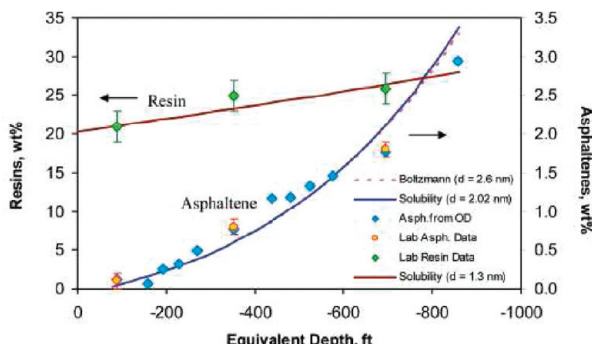


Figure 42. Asphaltene and resin gradients produced by centrifugation and fitted to a solubility model. Asphaltenes exhibit a huge gradient, while bulk resins exhibit a small gradient, indicating that bulk resins are definitely *not* associated with asphaltenes. The resin particle is found to be 1.3 nm, while the asphaltene nanoaggregate is found to be 2.0 nm.¹¹⁵

“this model (of resin–asphaltene association) has been adopted by succeeding generations of asphaltene researchers with little further examination, and its influence on subsequent research is difficult to overstate”.¹⁵⁴

Many different techniques have been discussed above that show asphaltenes stably suspended in toluene without resins; thus, resins are not necessary for stabilizing asphaltene colloidal particles in organic systems. Moreover, any stabilizing role of resins is unlikely to involve charge because they exhibit far less charge than asphaltenes.¹¹⁰ In addition, the asphaltene nanoaggregates found in crude oil appear very similar to those in toluene. For example, the flocculation properties of asphaltenes in crude oil are similar to those in model systems.¹⁵⁵ Nevertheless, the longstanding issue mandates a closer look.

The boundary between asphaltene and resin is defined within a chemical separation context and not a chemical classification. Moreover, the definition of asphaltenes varies somewhat, and the definition of resin varies to a greater extent. For separating asphaltenes, *n*-heptane is often defined as the precipitating solvent. *n*-Pentane is also used to define asphaltenes. The chemical fraction at the boundary between asphaltenes (for example, the *n*-pentane insolubles and *n*-heptane solubles) might be called the heaviest resins or the lightest asphaltenes depending upon which solvent is used to identify the asphaltenes. Consequently, the extent of asphaltene and resin interaction is dependent upon the exact definition used to identify the asphaltenes.¹⁵⁶

Recent centrifugation studies of a live crude oil have helped clarify the situation.¹¹⁵ Figure 42 shows that, in these experiments, a 10× gradient was obtained for asphaltenes (*n*-heptane insolubles), while the bulk resins exhibited a 25% gradient. Obviously, bulk resins are not bound with asphaltenes in a complex; otherwise, the gradients of bulk resins and asphaltenes would be comparable.

Nevertheless, the colored resins exhibit a factor of 2 gradient in these centrifugation experiments (Figure 43).¹¹⁵ This is smaller than the 10× gradient of asphaltenes but much larger than the 25% gradient of bulk resins. These observations can be explained in various ways, but the authors argued that the most likely explanation is that a fraction of the colored

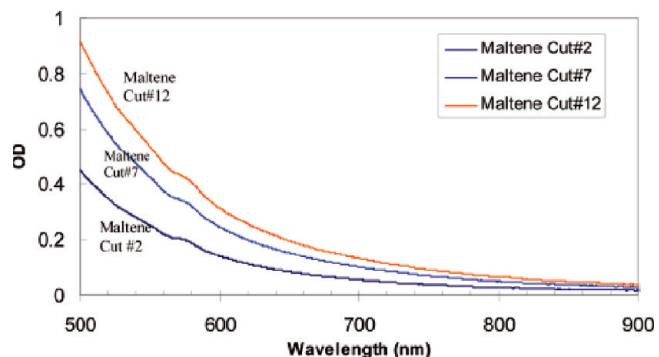


Figure 43. Optical spectra for the maltenes in *n*-heptane for samples near the top (2), middle (7), and bottom (12) of the centrifuge tube. The “colored” resins dominate the optical absorption of the maltenes and show a gradient of a factor of 2, a much smaller gradient than the asphaltenes but much larger than bulk resins.¹¹⁵

resins are associated in asphaltene nanoaggregates. A description consistent with the data is that there is one resin molecule per asphaltene nanoaggregate in the crude oil. On this issue, these results supersede other, less controllable gravitation segregation data of a live crude,¹¹⁶ in an oil reservoir where very little asphaltene–resin interaction was found.

In a live crude oil, only a small fraction of the asphaltene nanoaggregate is composed of resin. Moreover, the asphaltene nanoaggregates have very small aggregation numbers; therefore, they have a very large surface/volume ratio. If resins were going to act as surfactants to asphaltenes, thus coating the surface, then a large fraction of the nanoaggregate would need to be resin. The centrifugation of live crude oil shows that only a small fraction of the nanoaggregates is resins. The micelle model with surfactant resins is *not* a correct representation of asphaltene nanoaggregates. These data show that the resins do not act as a surfactant to the asphaltene nanoaggregates.

Ultrafiltration studies of very asphaltic systems initially found little evidence of asphaltene–resin interaction.¹³³ In these studies, *n*-pentane was used to define asphaltene; the more encompassing asphaltene definition necessarily yields a smaller quantity of interacting resins. Moreover, as shown by the centrifugation experiments, only a very small fraction of bulk resins participates in asphaltene aggregate formation. A comprehensive interpretation of all data from the ultrafiltration experiments on very asphaltic systems indicated that the extent of resin interaction with asphaltenes varies with conditions and is on the order of 15% by mass.¹⁵⁷ There could be differences for these very asphaltic systems compared to more conventional black oils; ultrafiltration finds larger colloidal particles for this asphaltic system even at ~200 °C¹³³ than other studies of nanofiltration for more conventional black oils at 80 °C.¹³⁴ In any event, some degree of asphaltene–resin interaction is found in both centrifugation and ultrafiltration.

Microcalorimetry results indicate there is an asphaltene–resin interaction and that the strength of interaction is 2–4 kJ/mol and comparable to the asphaltene–asphaltene interaction.^{130,158} This value of the enthalpy is noted to be comparable to some modeling analyses.¹⁵⁸ Other studies have

(155) Aske, N.; Kallevik, H.; Johnsen, E. E.; Sjøblom, J. Asphaltene aggregation from crude oils and model systems studied by high-pressure NMR spectroscopy. *Energy Fuels* 2002, 16, 1287–1295.

(156) Daniel Marino-Garcia has made the point correctly in our view in several conferences.

(157) Zhao, B.; Becerra, M.; Shaw, J. M. On asphaltene and resin association in Athabasca bitumen and Maya crude oil. *Energy Fuels* 2009, 23, 4431–4437.

(158) Merino-Garcia, D.; Andersen, S. I. Thermodynamic characterization of asphaltene–resin interaction by microcalorimetry. *Langmuir* 2004, 20, 4559–4565.

also seen effects from resins on asphaltene aggregation. SANS measurements indicate that asphaltene aggregate sizes decrease in the presence of resins.¹⁵⁹ This is consistent with the smaller complexing molecules acting as “chain terminators”, while the large, strongly complexing asphaltene molecules act as chain propagators.¹⁶⁰ These data are also consistent with the finding that the more soluble asphaltene fractions are characterized by smaller sized aggregates.¹⁶¹ The addition of resins to asphaltenes in toluene reduced the interfacial activity of the corresponding solutions.¹⁵⁹ The resins might act to bind high-energy sites that would otherwise be more available to be active at oil–water interfaces.¹⁵⁹ Other measurements also indicate that there are asphaltene–resin interactions, such as the measurement of vapor pressure osmometry.¹⁶² Asphaltenes absorb differently onto quartz crystal microbalances dependent upon whether resins are present.¹⁶³ There is evidently asphaltene–resin interactions. Nevertheless, the interaction is not properly framed within a micelle model, and the corresponding ubiquitous cartoons of resins stabilizing asphaltene nanoaggregates should no longer be reproduced.

8. Conclusions

The modified Yen model provides a first-principles framework to account for a tremendous volume of data acquired for asphaltenes at multiple length scales involving wide ranging methodologies and phenomena. The three components that

(159) Spiecker, P. M.; Gawrys, K. L.; Trail, C. B.; Kilpatrick, P. K. Effects of petroleum resins on asphaltene aggregation and water-in-oil emulsion formation. *Colloids Surf., A* **2003**, *220*, 9–27.

(160) Agrawala, M.; Yarranton, H. W. Asphaltene association model analogous to linear polymerization. *Ind. Eng. Chem. Res.* **2001**, *40*, 4664–4672.

(161) Fossen, M.; Kallevik, H.; Knudsen, K. D.; Sjöblom, J. Asphaltenes precipitated by a two-step precipitation procedure. I. Interfacial tension and solvent properties. *Energy Fuels* **2007**, *21*, 1030–1037.

(162) Yarranton, H. W.; Fox, W. A.; Svcek, W. Y. Effects of resins on asphaltene self-association and solubility. *Can. J. Chem. Eng.* **2007**, *85*, 635–642.

(163) Ekholm, P.; Blomberg, E.; Claesson, P.; Auflem, I. H.; Sjöblom, J.; Kornfeldt, A. A quartz crystal microbalance study of the adsorption of asphaltenes and resins onto a hydrophilic surface. *J. Colloid Interface Sci.* **2002**, *247*, 342–350.

comprise the modified Yen model are asphaltene molecules, asphaltene nanoaggregates, and clusters of asphaltene nanoaggregates. The foundation of the modified Yen model is the resolution of understanding the asphaltene molecular architecture, thereby enabling development of structure–function relationships. The dynamics, the concentrations of formations of these aggregate species, are implicit in the modified Yen model. The development of this model signifies in large measure the resolution of many controversies that have plagued the field of asphaltene science. In our view, explicitly framing future asphaltene studies within the modified Yen model will improve efficiency of progress in the field. Indeed, the modified Yen model has already proven its mettle in addressing very challenging problems, such as asphaltene interfacial science. So often, development of new technology coupled with new science produces enormous benefits. The new technology DFA coupled with the modified Yen model has been successfully applied to understand compositional gradients in oilfield reservoirs. Reservoir connectivity, the industry’s largest technical risk factor, is routinely analyzed within predictive models applied to condensates and volatile oils. The modified Yen model with DFA provides the capability to extend connectivity analyses to black oils as well as providing a new framework for corresponding analyses of reservoir condensates. The modified Yen model represents the culmination of extraordinary effort by numerous contributors and provides a congruent foundation for the future of the field, enabling focus on the most important issues in the petroleum industry.

Acknowledgment. First and foremost, the author is very grateful to his many gifted students. Without their dedication and skill, the author’s vision never would have come to fruition. The author is indebted to his numerous collaborators who, with their unique capabilities, have contributed greatly to the field and to this author specifically. The author gratefully acknowledges his many colleagues who have helped shape his evolving perspective. In addition, the author also acknowledges all those who engaged in the vigorous and, at times, pointed debates that have helped identify important issues to be resolved and helped focus the energies of the discipline.